

Distributionally Robust Kalman Filter*

Minhyuk Jang, Astghik Hakobyan, and Insoon Yang[‡]

Abstract

We study state estimation for discrete-time linear stochastic systems under distributional ambiguity in the initial state, process noise, and measurement noise. We propose a noise-centric distributionally robust Kalman filter (DRKF) based on Wasserstein ambiguity sets imposed directly on these distributions. This formulation excludes dynamically unreachable priors and yields a Kalman-type recursion driven by least-favorable covariances computed via semidefinite programs (SDP). In the time-invariant case, the steady-state DRKF is obtained from a *single* stationary SDP, producing a constant gain with Kalman-level online complexity. We establish the convergence of the DR Riccati covariance iteration to the stationary SDP solution, together with an explicit sufficient condition for a prescribed convergence rate. We further show that the proposed noise-centric model induces *a priori* spectral bounds on all feasible covariances and a Kalman filter sandwiching property for the DRKF covariances. Finally, we prove that the steady-state error dynamics are Schur stable, and the steady-state DRKF is asymptotically minimax optimal with respect to worst-case mean-square error.

1 Introduction

State estimation is a fundamental problem in systems and control, where the objective is to infer the system state from noisy and partial measurements. For linear systems with Gaussian noise and known statistics, the Kalman filter (KF) [2] provides the optimal minimum mean-square error (MMSE) estimator. In practice, however, noise statistics are rarely known *a priori*: they are typically learned from limited data, subject to modeling error, and may vary over time. Even moderate misspecification can significantly degrade estimation performance, while severe mismatch may lead to divergence.

To mitigate this sensitivity, several robust estimation frameworks have been developed. The H_∞ filter [3] guarantees bounded estimation error under worst-case disturbances, but it is often conservative in stochastic settings. Risk-sensitive filters (e.g., [4] and [5]) penalize large errors exponentially via an entropic risk measure, but their performance relies on an accurate specification of the underlying noise distributions, which may be difficult to justify in practice.

In contrast, recent advances in distributionally robust optimization (DRO) have motivated growing interest in *distributionally robust state estimation* (DRSE). In DRSE, the true noise distributions are

*This work was supported in part by the Information and Communications Technology Planning and Evaluation (IITP) grant funded by MSIT(2022-0-00124, 2022-0-00480). The work of A. Hakobyan was supported in part by the Higher Education and Science Committee of RA (Research project 24IRF-2B002).

[†]The first two authors contributed equally. A preliminary version of this paper was presented at the 2025 IEEE Conference on Decision and Control [1].

[‡]M. Jang is with the Department of Mechanical Science and Engineering, Grainger College of Engineering, University of Illinois Urbana-Champaign, Urbana, IL, United States jang64@illinois.edu. A. Hakobyan is with the Center for Scientific Innovation and Education and National Polytechnic University of Armenia, Yerevan, Armenia astghik.hakobyan@csie.am. I. Yang is with the Department of Electrical and Computer Engineering and ASRI, Seoul National University, Seoul, South Korea insoonyang@snu.ac.kr.

assumed to lie in an ambiguity set centered at a nominal model, and the estimator minimizes the worst-case expected error over this set. While distributional robustness has been extensively studied in control design (e.g., [6–12]), its application to state estimation remains comparatively limited.

Existing DRSE formulations vary along two key dimensions: (i) the *geometry* of the ambiguity set, such as ϕ -divergence balls, moment-based sets [13–16], or Wasserstein balls [17–21]; and (ii) the *location* where ambiguity is imposed, e.g., on the joint state–measurement distribution [17], on the prior state and measurement noise [18], or via bicausal optimal transport models that encode temporal dependence [20]. These choices have significant implications for tractability, interpretability, and long-term behavior.

Despite this progress, *steady-state* DRSE remains underdeveloped. For long-horizon operation, constant-gain estimators with fixed offline complexity are essential. However, many existing time-varying DRKFs require solving an optimization problem at each time step, or lead to horizon-dependent formulations whose size grows with time. While the frequency-domain minimax approach of [21] characterizes an optimal linear time-invariant estimator, the resulting filter is generally non-rational and does not admit a finite-dimensional state-space realization.

The preliminary version [1] of this work derived a steady-state DRKF by placing ambiguity sets on the prior state and measurement noise distributions. In this paper, we substantially extend this line of work by adopting a *noise-centric* formulation, in which Wasserstein ambiguity sets are imposed directly on the initial state, process noise, and measurement noise distributions. This modeling choice enforces a form of *dynamic consistency*: all admissible prior distributions arise through propagation of the system dynamics under admissible noise realizations. Moreover, it admits a finite-dimensional steady-state characterization and yields a constant-gain DRKF from a *single* stationary semidefinite program (SDP), while providing several theoretical and computational advantages.

Our main contributions are summarized as follows.

- **Noise-centric ambiguity modeling.** We define Wasserstein ambiguity sets directly on the initial state, process noise, and measurement noise distributions. This modeling choice enforces *dynamic consistency*, ensuring that all admissible prior distributions arise through propagation of the system dynamics under admissible noise realizations, and forms the structural basis for the subsequent theoretical and algorithmic developments.
- **Steady-state DRKF via a single stationary SDP.** In the time-invariant setting, we obtain a constant-gain steady-state DRKF by solving a *single* stationary SDP offline, yielding Kalman-level per-step online complexity.
- **Convergence with explicit rate conditions.** We establish the convergence of the DR Riccati iteration governing the state-error covariance to a unique steady-state solution characterized by the stationary SDP. Moreover, we derive an explicit sufficient condition on the ambiguity radii that guarantees a *prescribed* contraction rate.
- **Spectral structure and steady-state guarantees.** We show that Wasserstein ambiguity induces explicit *a priori* eigenvalue bounds (an *eigenvalue tube*) and a KF-sandwich property for the DRKF covariances. We further establish Schur stability of the steady-state estimation error dynamics and asymptotic minimax optimality with respect to the worst-case mean-square error (MSE).

The remainder of the paper is organized as follows. Section 2 introduces the problem formulation and Wasserstein ambiguity sets. Section 3 presents the finite-horizon and steady-state DRKF constructions and their SDP reformulations. Section 4 develops spectral boundedness, convergence,

stability, and optimality results. Section 5 illustrates the performance of the proposed methods through numerical experiments.

2 Problem Setup

Notation. Let \mathbb{S}^n denote the set of symmetric matrices in $\mathbb{R}^{n \times n}$, and let \mathbb{S}_+^n and \mathbb{S}_{++}^n be the positive semidefinite and positive definite cones. For $A, B \in \mathbb{S}^n$, write $A \succeq B$ (resp. $A \succ B$) if $A - B \in \mathbb{S}_+^n$ (resp. \mathbb{S}_{++}^n). For a matrix A , $\|A\|_2$ and $\|A\|_F$ denote the spectral and Frobenius norms. For $A \in \mathbb{S}^n$, $\lambda_{\min}(A)$ and $\lambda_{\max}(A)$ denote its smallest and largest eigenvalues, while $\sigma_{\min}(A)$ and $\sigma_{\max}(A)$ denote its smallest and largest singular values. Let $\mathcal{P}(\mathcal{W})$ be the set of Borel probability measures supported on $\mathcal{W} \subseteq \mathbb{R}^n$, and let $\mathcal{P}_2(\mathcal{W})$ be those with finite second moments. For probability measures \mathbb{P}, \mathbb{Q} , their product measure is denoted by $\mathbb{P} \otimes \mathbb{Q}$. Let $\mathbf{1}_N \in \mathbb{R}^N$ denote the vector of all ones, and let $\text{blkdiag}(A_1, \dots, A_N)$ denote the block-diagonal matrix with diagonal blocks A_1, \dots, A_N .

2.1 Distributionally Robust State Estimation Problem

Consider the discrete-time linear stochastic system¹

$$\begin{aligned} x_{t+1} &= A_t x_t + w_t, \\ y_t &= C_t x_t + v_t, \end{aligned} \tag{1}$$

where $x_t \in \mathbb{R}^{n_x}$ and $y_t \in \mathbb{R}^{n_y}$ denote the system state and output. The process noise $w_t \in \mathbb{R}^{n_x}$ and measurement noise $v_t \in \mathbb{R}^{n_y}$ follow distributions $\mathbb{Q}_{w,t} \in \mathcal{P}(\mathbb{R}^{n_x})$ and $\mathbb{Q}_{v,t} \in \mathcal{P}(\mathbb{R}^{n_y})$, while the initial state x_0 follows $\mathbb{Q}_{x,0} \in \mathcal{P}(\mathbb{R}^{n_x})$. We assume that x_0 , $\{w_t\}$, and $\{v_t\}$ are mutually independent, and that each of $\{w_t\}$ and $\{v_t\}$ is temporally independent.²

At each time $t \geq 0$, the estimator has access to the measurement history $\mathcal{Y}_t := \{y_0, \dots, y_t\}$. The goal is to estimate x_t given \mathcal{Y}_t . A natural criterion is the conditional minimum mean-square error (MMSE),

$$\min_{\psi_t \in \mathcal{F}_t} J_t(\psi_t, \mathbb{Q}_{e,t}) := \mathbb{E} [\|x_t - \psi_t(\mathcal{Y}_t)\|^2 \mid \mathcal{Y}_{t-1}], \tag{2}$$

where \mathcal{F}_t denotes the set of measurable estimators $\psi_t : (\mathbb{R}^{n_y})^{t+1} \rightarrow \mathbb{R}^{n_x}$. That is, ψ_t minimizes the conditional mean-square estimation error given past observations.

For $t > 0$, the conditional distribution of (x_t, y_t) given \mathcal{Y}_{t-1} is fully determined by the posterior distribution $\mathbb{P}_{x,t-1}$ of x_{t-1} and the joint noise distribution $\mathbb{Q}_{e,t} := \mathbb{Q}_{w,t-1} \otimes \mathbb{Q}_{v,t}$. At $t = 0$, no posterior from a previous step exists. We adopt the convention $\mathcal{Y}_{-1} = \emptyset$ and define $\mathbb{P}_{x,0}^- := \mathbb{Q}_{x,0}$ and $\mathbb{Q}_{e,0} := \mathbb{P}_{x,0}^- \otimes \mathbb{Q}_{v,0}$, so that (2) also covers the initial stage.³

When $x_0 \sim \mathcal{N}(\hat{x}_0^-, \Sigma_{x,0}^-)$ and $\{w_t\}, \{v_t\}$ are independent Gaussian sequences with known covariances, the optimal causal MMSE estimator reduces to the classical KF. In practice, however, noise statistics are typically estimated from limited data and are thus subject to ambiguity. In practice, only nominal distributions $\hat{\mathbb{Q}}_{w,t}$, $\hat{\mathbb{Q}}_{v,t}$, and $\hat{\mathbb{Q}}_{x,0}$ are available from identification procedures (e.g., [23, 24]).⁴ Even modest deviations between nominal and true distributions can significantly degrade performance

¹Throughout, we assume that the system matrices A_t and C_t are known, and we focus exclusively on uncertainty in the noise statistics.

²Such independence assumptions are standard in the control and estimation literature; see, e.g., [22, Sect. 2.2] and [3, Sect. 5.1].

³We use the superscript “ $-$ ” for prior quantities; e.g., \bar{x}_t^- , $\Sigma_{x,t}^-$, and $\mathbb{P}_{x,t}^-$ denote the prior mean, covariance, and distribution of x_t conditioned on \mathcal{Y}_{t-1} .

⁴A hat, $\hat{\cdot}$, denotes nominal quantities; e.g., \hat{x}_0^- and $\hat{\mathbb{Q}}_{x,0}$ represent the nominal initial state mean and distribution, respectively.

or cause divergence, especially when disturbances accumulate over time (e.g., marginally stable or unstable systems).

To address this, we formulate a stage-wise minimax problem in which the estimator competes against an adversary that selects distributions from ambiguity sets $\mathbb{D}_{j,t} \subset \mathcal{P}(\mathbb{R}^{n_j})$ for $j \in \{w, v, x\}$ to be defined later. The resulting DRSE problem at time t is

$$\min_{\psi_t \in \mathcal{F}_t} \max_{\mathbb{P}_{e,t} \in \mathbb{D}_{e,t}} J_t(\psi_t, \mathbb{P}_{e,t}), \quad (3)$$

where $\mathbb{D}_{e,0} := \mathbb{D}_{x,0} \times \mathbb{D}_{v,0}$ and $\mathbb{D}_{e,t} := \mathbb{D}_{w,t-1} \times \mathbb{D}_{v,t}$ for $t > 0$. The corresponding joint distributions are $\mathbb{P}_{e,0} := \mathbb{P}_{x,0}^- \otimes \mathbb{P}_{v,0}$ and $\mathbb{P}_{e,t} := \mathbb{P}_{w,t-1} \otimes \mathbb{P}_{v,t}$, reflecting the assumed stage-wise independence between process and measurement noise.

Remark 1. *In contrast to formulations that place ambiguity on a joint prior state-measurement distribution (e.g., [1, 18]), our approach imposes ambiguity directly on the noise distributions. This enforces a form of dynamic consistency: admissible priors arise only through the system dynamics (1) under admissible noise realizations. By contrast, previous DRSE formulations may allow priors that are not dynamically reachable. Our formulation also allows the adversary to couple estimation performance across time, capturing long-term accumulation of disturbances via the state recursion, even though the ambiguity sets themselves are stage-wise. For systems with slow or unstable dynamics, even small biases in w_t can lead to unbounded state growth, making this sequential robustness essential.*

2.2 Wasserstein Ambiguity Sets

We adopt Wasserstein ambiguity sets due to their favorable analytical properties and their ability to exclude statistically irrelevant distributions (e.g., [25, 26]). The *type-2 Wasserstein distance* between two probability distributions $\mathbb{P}, \mathbb{Q} \in \mathcal{P}(\mathcal{W})$ is defined as

$$W_2(\mathbb{P}, \mathbb{Q}) := \inf_{\tau \in \mathcal{T}(\mathbb{P}, \mathbb{Q})} \left\{ \left(\int_{\mathcal{W} \times \mathcal{W}} \|x - y\|^2 d\tau(x, y) \right)^{\frac{1}{2}} \right\},$$

where $\mathcal{T}(\mathbb{P}, \mathbb{Q})$ denotes the set of joint probability measures with marginals \mathbb{P} and \mathbb{Q} . The optimization variable τ represents the *transportation plan* that redistributes probability mass from \mathbb{P} to \mathbb{Q} .⁵

We define the ambiguity sets as Wasserstein balls centered at nominal distributions: for $j \in \{w, v, x_0\}$,

$$\mathbb{D}_{j,t} := \{ \mathbb{P}_{j,t} \in \mathcal{P}(\mathbb{R}^{n_j}) \mid W_2(\mathbb{P}_{j,t}, \hat{\mathbb{Q}}_{j,t}) \leq \theta_j \},$$

where θ_j specifies the robustness radius.⁶

In general, computing W_2 is difficult. A useful surrogate is the *Gelbrich distance*. Specifically, the Gelbrich distance between $\mathbb{P} \in \mathcal{P}(\mathbb{R}^n)$ and $\mathbb{Q} \in \mathcal{P}(\mathbb{R}^n)$ with mean vectors $\mu_1, \mu_2 \in \mathbb{R}^n$ and covariance matrices $\Sigma_1, \Sigma_2 \in \mathbb{S}_+^n$ is defined as

$$G(\mathbb{P}, \mathbb{Q}) := \sqrt{\|\mu_1 - \mu_2\|_2^2 + \mathcal{B}^2(\Sigma_1, \Sigma_2)},$$

where $\mathcal{B}(\Sigma_1, \Sigma_2) := \sqrt{\text{Tr}[\Sigma_1 + \Sigma_2 - 2(\Sigma_2^{\frac{1}{2}} \Sigma_1 \Sigma_2^{\frac{1}{2}})^{\frac{1}{2}}]}$ is the *Bures-Wasserstein distance*.

The Gelbrich distance always provides a lower bound on the type-2 Wasserstein distance, i.e., $G(\mathbb{P}, \mathbb{Q}) \leq W_2(\mathbb{P}, \mathbb{Q})$. Moreover, equality holds when both distributions are Gaussian, or, more generally, elliptical with the same density generator [27].

⁵We use the Euclidean norm to measure the transportation cost $\|x - y\|$.

⁶The formulation can be extended to correlated noise by placing a single Wasserstein ball around the joint distribution, at the cost of higher-dimensional optimization problems.

3 Distributionally Robust Kalman Filters

We develop tractable DR state estimators consistent with the noise-centric ambiguity model in Section 2. We first present a finite-horizon formulation whose recursion mirrors that of the classical KF when driven by least-favorable noise covariances. We then specialize to the time-invariant case and derive a steady-state DRKF obtained from a *single* stationary SDP, yielding a constant-gain filter with Kalman-level online complexity.

3.1 Finite-Horizon Case

We begin with a standard assumption on the nominal distributions that ensures tractability of the DRSE problem and preserves the affine–Gaussian structure underlying closed-form KF updates.

Assumption 1. *The nominal distributions of the initial state x_0 , process noise w_t , and measurement noise v_t are Gaussian for all t , i.e., $\hat{\mathbb{Q}}_{x,0} = \mathcal{N}(\hat{x}_0^-, \hat{\Sigma}_{x,0}^-)$, $\hat{\mathbb{Q}}_{w,t} = \mathcal{N}(\hat{w}_t, \hat{\Sigma}_{w,t})$, and $\hat{\mathbb{Q}}_{v,t} = \mathcal{N}(\hat{v}_t, \hat{\Sigma}_{v,t})$ with mean vectors $\hat{x}_0^- \in \mathbb{R}^{n_x}$, $\hat{w}_t \in \mathbb{R}^{n_x}$, and $\hat{v}_t \in \mathbb{R}^{n_y}$ and covariance matrices $\hat{\Sigma}_{x,0}^- \in \mathbb{S}_+^{n_x}$, $\hat{\Sigma}_{w,t} \in \mathbb{S}_+^{n_x}$, $\hat{\Sigma}_{v,t} \in \mathbb{S}_{++}^{n_y}$, respectively.*

Under this assumption, the DRSE problem (3) admits the following convex reformulations.

Lemma 1. *Suppose Assumption 1 holds. Then, the DRSE problem (3) satisfies the following properties.*

(i) *At the initial stage, the following convex optimization problem has the same optimal value as (3), and any of its optimal solutions are optimal for (3):*

$$\begin{aligned} & \max_{\Sigma_{x,0}^-, \Sigma_{v,0}} \text{Tr}[\Sigma_{x,0}^- - \Sigma_{x,0}^- C_0^\top (C_0 \Sigma_{x,0}^- C_0^\top + \Sigma_{v,0})^{-1} C_0 \Sigma_{x,0}^-] \\ & \text{s.t. } \text{Tr}[\Sigma_{x,0}^- + \hat{\Sigma}_{x,0}^- - 2((\hat{\Sigma}_{x,0}^-)^{\frac{1}{2}} \Sigma_{x,0}^- (\hat{\Sigma}_{x,0}^-)^{\frac{1}{2}})^{\frac{1}{2}}] \leq \theta_{x_0}^2 \\ & \quad \text{Tr}[\Sigma_{v,0} + \hat{\Sigma}_{v,0} - 2((\hat{\Sigma}_{v,0}^{\frac{1}{2}} \Sigma_{v,0} \hat{\Sigma}_{v,0}^{\frac{1}{2}})^{\frac{1}{2}})] \leq \theta_v^2 \\ & \quad \Sigma_{x,0}^- \succeq \lambda_{\min}(\hat{\Sigma}_{x,0}^-) I_{n_x}, \quad \Sigma_{v,0} \succeq \lambda_{\min}(\hat{\Sigma}_{v,0}) I_{n_y} \\ & \quad \Sigma_{x,0}^- \in \mathbb{S}_+^{n_x}, \quad \Sigma_{v,0} \in \mathbb{S}_+^{n_y}. \end{aligned} \tag{4}$$

(ii) *For any $t > 0$, fix the state distribution $\mathbb{P}_{x,t-1} = \mathcal{N}(\bar{x}_{t-1}, \Sigma_{x,t-1})$. Then the following convex optimization problem has the same optimal value as (3), and any of its optimal solutions are optimal for (3):*

$$\begin{aligned} & \max_{\Sigma_{w,t-1}, \Sigma_{v,t}} \text{Tr}[\Sigma_{x,t}^- - \Sigma_{x,t}^- C_t^\top (C_t \Sigma_{x,t}^- C_t^\top + \Sigma_{v,t})^{-1} C_t \Sigma_{x,t}^-] \\ & \text{s.t. } \text{Tr}[\Sigma_{w,t-1} + \hat{\Sigma}_{w,t-1} - 2((\hat{\Sigma}_{w,t-1}^{\frac{1}{2}} \Sigma_{w,t-1} \hat{\Sigma}_{w,t-1}^{\frac{1}{2}})^{\frac{1}{2}})] \leq \theta_w^2 \\ & \quad \text{Tr}[\Sigma_{v,t} + \hat{\Sigma}_{v,t} - 2((\hat{\Sigma}_{v,t}^{\frac{1}{2}} \Sigma_{v,t} \hat{\Sigma}_{v,t}^{\frac{1}{2}})^{\frac{1}{2}})] \leq \theta_v^2 \\ & \quad \Sigma_{x,t}^- = A_{t-1} \Sigma_{x,t-1} A_{t-1}^\top + \Sigma_{w,t-1} \\ & \quad \Sigma_{w,t-1} \succeq \lambda_{\min}(\hat{\Sigma}_{w,t-1}) I_{n_x}, \quad \Sigma_{v,t} \succeq \lambda_{\min}(\hat{\Sigma}_{v,t}) I_{n_y} \\ & \quad \Sigma_{x,t}^-, \Sigma_{w,t-1} \in \mathbb{S}_+^{n_x}, \quad \Sigma_{v,t} \in \mathbb{S}_+^{n_y}. \end{aligned} \tag{5}$$

(iii) *If $(\Sigma_{x,0}^*, \Sigma_{v,0}^*)$ and $(\Sigma_{w,t-1}^*, \Sigma_{v,t}^*)$ solve (4) and (5), respectively, then the maximum in (3) is attained by the Gaussian distributions $\mathbb{P}_{x,0}^* = \mathcal{N}(\hat{x}_0^-, \Sigma_{x,0}^*)$, $\mathbb{P}_{w,t-1}^* = \mathcal{N}(\hat{w}_{t-1}, \Sigma_{w,t-1}^*)$ and $\mathbb{P}_{v,t}^* =$*

$\mathcal{N}(\hat{v}_t, \Sigma_{v,t}^*)$ for each t . Furthermore, the minimax-optimal estimator is affine and given by

$$\psi_t^*(\mathcal{Y}_t) = \bar{x}_t^- + \Sigma_{x,t}^- C_t^\top (C_t \Sigma_{x,t}^- C_t^\top + \Sigma_{v,t}^*)^{-1} (y_t - C_t \bar{x}_t^- - \hat{v}_t), \quad (6)$$

with $\bar{x}_t^- = A_{t-1} \bar{x}_{t-1} + \hat{w}_{t-1}$, $\Sigma_{x,t}^- = A_{t-1} \Sigma_{x,t-1} A_{t-1}^\top + \Sigma_{w,t-1}^*$, and $\Sigma_{x,0}^- = \Sigma_{x,0}^{-,*}$, $\bar{x}_0^- = \hat{x}_0^-$.

Problems (4) and (5) define the stage-wise minimax interaction: the estimator selects ψ_t , while the adversary selects noise covariances within Wasserstein balls. Problem (4) yields the least-favorable prior and measurement covariances $(\Sigma_{x,0}^{-,*}, \Sigma_{v,0}^*)$ at $t = 0$, whereas (5) yields the least-favorable process and measurement covariances $(\Sigma_{w,t-1}^*, \Sigma_{v,t}^*)$ for $t \geq 1$. The corresponding optimal values represent the least-favorable posterior MSE at each stage.

Lemma 1 extends [18, Thm. 3.1] to the noise-centric setting by replacing ambiguity on the prior state (for $t > 0$) with ambiguity on the process noise. Although the Wasserstein constraints are equivalently expressible in terms of first and second moments, this does not meaningfully restrict the adversary under Assumption 1. For Gaussian nominal distributions, the least-favorable distributions are Gaussian, and the worst-case behavior is fully characterized by their means and covariances. Furthermore, even without Gaussian nominal assumptions, (6) remains minimax optimal within the class of affine estimators [18].

Remark 2. *Although the ambiguity sets are defined as W_2 balls over full distributions, the maximization problems in (4) and (5) admit least-favorable distributions that preserve the nominal noise means. Indeed, for any fixed distribution, the minimizing estimator is the conditional mean, and the conditional MSE depends only on the posterior covariance through its trace. Mean shifts consume Wasserstein budget without increasing the worst-case MSE as effectively as perturbing the covariance. Hence, mean shifts are suboptimal for the adversary, and the ambiguity budget is used entirely to perturb covariances, as reflected in Lemma 1 and Theorem 1.*

Remark 3. *By adapting the structural argument used in [18, Lemma A.3], the DRSE problem (3) admits at least one maximizer whose covariance matrices satisfy $\Sigma_{x,0}^{-,*} \succeq \lambda_{\min}(\hat{\Sigma}_{x,0}^-) I_{n_x}$, $\Sigma_{v,0}^* \succeq \lambda_{\min}(\hat{\Sigma}_{v,0}) I_{n_y}$, for $t = 0$, and $\Sigma_{w,t-1}^* \succeq \lambda_{\min}(\hat{\Sigma}_{w,t-1}) I_{n_x}$, $\Sigma_{v,t}^* \succeq \lambda_{\min}(\hat{\Sigma}_{v,t}) I_{n_y}$ for all $t > 0$ (see Appendix A). Because such a maximizer always exists, the explicit eigenvalue lower-bound constraints in (4) and (5) are redundant: they do not alter the optimal value but only restrict attention to maximizers that satisfy these bounds. Equivalently, removing these constraints yields problems with the same optimal value as (3).*

Both problems (4) and (5) are solvable for $\hat{\Sigma}_{v,t} \in \mathbb{S}_{++}^{n_y}$ since their objectives are continuous over compact feasible sets. Applying the standard Schur complement argument, these problems reduce to SDPs that can be solved efficiently using off-the-shelf solvers.

Corollary 1. *Suppose Assumption 1 holds. Then, for any time $t > 0$, the optimization problem (5)*

is equivalent to the following tractable convex SDP:

$$\begin{aligned}
& \max_{\Sigma_{x,t}^-, \Sigma_{x,t}, \Sigma_{w,t-1}, \Sigma_{v,t}, Y, Z} \text{Tr}[\Sigma_{x,t}] \\
& \text{s.t. } \begin{bmatrix} \Sigma_{x,t}^- - \Sigma_{x,t} & \Sigma_{x,t}^- C_t^\top \\ C_t \Sigma_{x,t}^- & C_t \Sigma_{x,t}^- C_t^\top + \Sigma_{v,t} \end{bmatrix} \succeq 0 \\
& \begin{bmatrix} \hat{\Sigma}_{w,t-1} & Y \\ Y^\top & \Sigma_{w,t-1} \end{bmatrix} \succeq 0, \quad \begin{bmatrix} \hat{\Sigma}_{v,t} & Z \\ Z^\top & \Sigma_{v,t} \end{bmatrix} \succeq 0 \\
& \text{Tr}[\Sigma_{w,t-1} + \hat{\Sigma}_{w,t-1} - 2Y] \leq \theta_w^2 \\
& \text{Tr}[\Sigma_{v,t} + \hat{\Sigma}_{v,t} - 2Z] \leq \theta_v^2 \\
& \Sigma_{x,t}^- = A_{t-1} \Sigma_{x,t-1} A_{t-1}^\top + \Sigma_{w,t-1} \\
& \Sigma_{w,t-1} \succeq \lambda_{\min}(\hat{\Sigma}_{w,t-1}) I_{n_x}, \quad \Sigma_{v,t} \succeq \lambda_{\min}(\hat{\Sigma}_{v,t}) I_{n_y} \\
& \Sigma_{x,t}^-, \Sigma_{x,t}, \Sigma_{w,t-1} \in \mathbb{S}_+^{n_x}, \quad \Sigma_{v,t} \in \mathbb{S}_+^{n_y} \\
& Y \in \mathbb{R}^{n_x \times n_x}, \quad Z \in \mathbb{R}^{n_y \times n_y}.
\end{aligned} \tag{7}$$

Similar results hold for $t = 0$. Solving (7) offline for all $t > 0$ yields the least-favorable covariances $(\Sigma_{w,t-1}^*, \Sigma_{v,t}^*)$. The next theorem shows that these covariances can be used directly in a Kalman-style recursion, resulting in a DR state estimator that is robust to distributional uncertainty.

Theorem 1 (DR Kalman Filter). *Under Assumption 1, the minimax-optimal DR state estimate $\psi_t^*(\mathcal{Y}_t)$ at any time t coincides with the conditional mean \bar{x}_t under the least-favorable distributions. Moreover, the least-favorable prior and posterior remain Gaussian: $\mathbb{P}_{x,t}^{-,*} = \mathcal{N}(\bar{x}_t^-, \Sigma_{x,t}^-)$, $\mathbb{P}_{x,t}^* = \mathcal{N}(\bar{x}_t, \Sigma_{x,t})$. These distributions are recursively computed for $t = 0, 1, \dots$ as follows:*

- **(Measurement Update)** Compute the DR Kalman gain

$$K_t = \Sigma_{x,t}^- C_t^\top (C_t \Sigma_{x,t}^- C_t^\top + \Sigma_{v,t}^*)^{-1}, \tag{8}$$

where $\Sigma_{v,t}^*$ is the maximizer of (5) for $t > 0$ and (4) for $t = 0$. Then, update \bar{x}_t and $\Sigma_{x,t}$ as

$$\bar{x}_t = K_t (y_t - C_t \bar{x}_t^- - \hat{v}_t) + \bar{x}_t^- \tag{9}$$

$$\Sigma_{x,t} = (I - K_t C_t) \Sigma_{x,t}^-. \tag{10}$$

The initial values are $\bar{x}_0^- = \hat{x}_0^-, \Sigma_{x,0}^- = \Sigma_{x,0}^{-,*}$, where $\Sigma_{x,0}^{-,*}$ is the maximizer of (4) at $t = 0$.

- **(State Prediction)** Predict \bar{x}_{t+1}^- and $\Sigma_{x,t+1}^-$ as

$$\bar{x}_{t+1}^- = A_t \bar{x}_t + \hat{w}_t \tag{11}$$

$$\Sigma_{x,t+1}^- = A_t \Sigma_{x,t} A_t^\top + \Sigma_{w,t}^*, \tag{12}$$

where $\Sigma_{w,t}^*$ is the maximizer of (5) at time $t + 1$.

Notably, the measurement update and state prediction equations (9)–(12) mirror those of the classical KF when the system is driven by the least-favorable distributions.

3.2 Infinite-Horizon Case

While the DRKF in Theorem 1 provides a tractable solution to the finite-horizon DRSE problem, our primary interest lies in its long-term behavior. To study this regime, we assume that both the system dynamics and the nominal uncertainty statistics are time-invariant.

Assumption 2. *The system (1) is time-invariant, i.e., $A_t \equiv A, C_t \equiv C$. Moreover, the nominal uncertainty distributions are stationary, so that $\hat{w}_t \equiv \hat{w}, \hat{v}_t \equiv \hat{v}$ and $\hat{\Sigma}_{v,t} \equiv \hat{\Sigma}_v, \hat{\Sigma}_{w,t} \equiv \hat{\Sigma}_w$ for all $t \geq 0$, where $\hat{\Sigma}_w \in \mathbb{S}_{++}^{n_x}$ and $\hat{\Sigma}_v \in \mathbb{S}_{++}^{n_y}$. The nominal initial state covariance satisfies $\hat{\Sigma}_{x,0}^- \in \mathbb{S}_{++}^{n_x}$.*

Under Assumption 2, the stage-wise SDPs (5)–(7) reduce to a time-invariant recursion for the covariance matrices. The resulting sequences of least-favorable noise covariances $\{\Sigma_{w,t}^*, \Sigma_{v,t}^*\}$ and state covariances $\{\Sigma_{x,t}^-, \Sigma_{x,t}\}$ may converge to limiting values $\{\Sigma_{w,\infty}, \Sigma_{v,\infty}\}$ and $\{\Sigma_{x,\infty}^-, \Sigma_{x,\infty}\}$ as $t \rightarrow \infty$. Whether such convergence holds depends on additional conditions, which are established later in Section 4.2. Motivated by this, we seek a steady-state DR estimator with a constant gain.

In the infinite-horizon setting, the DRSE problem reduces to computing these steady-state covariances and the associated DR Kalman gain. Since the dynamics and nominal statistics are time-invariant, the stage-wise SDP (5) simplifies to the following convex program:

$$\begin{aligned}
& \max_{\Sigma_{w,\infty}, \Sigma_{v,\infty}, \Sigma_{x,\infty}^-} \text{Tr}[\Sigma_{x,\infty}] \\
\text{s.t. } & \Sigma_{x,\infty} = \Sigma_{x,\infty}^- - \Sigma_{x,\infty}^- C^\top (C \Sigma_{x,\infty}^- C^\top + \Sigma_{v,\infty})^{-1} C \Sigma_{x,\infty}^- \\
& \Sigma_{x,\infty}^- = A \Sigma_{x,\infty} A^\top + \Sigma_{w,\infty} \\
& \text{Tr}[\Sigma_{w,\infty} + \hat{\Sigma}_w - 2(\hat{\Sigma}_w^{\frac{1}{2}} \Sigma_{w,\infty} \hat{\Sigma}_w^{\frac{1}{2}})^{\frac{1}{2}}] \leq \theta_w^2 \\
& \text{Tr}[\Sigma_{v,\infty} + \hat{\Sigma}_v - 2(\hat{\Sigma}_v^{\frac{1}{2}} \Sigma_{v,\infty} \hat{\Sigma}_v^{\frac{1}{2}})^{\frac{1}{2}}] \leq \theta_v^2 \\
& \Sigma_{w,\infty} \succeq \lambda_{\min}(\hat{\Sigma}_w) I_{n_x}, \Sigma_{v,\infty} \succeq \lambda_{\min}(\hat{\Sigma}_v) I_{n_y} \\
& \Sigma_{x,\infty}^-, \Sigma_{x,\infty}, \Sigma_{w,\infty} \in \mathbb{S}_{++}^{n_x}, \Sigma_{v,\infty} \in \mathbb{S}_{++}^{n_y}.
\end{aligned}$$

As in the finite-horizon case, this problem admits an equivalent SDP formulation. In particular, it can be written as the following *single* stationary SDP:

$$\begin{aligned}
& \max_{\Sigma_{x,\infty}^-, \Sigma_{x,\infty}, \Sigma_{w,\infty}, \Sigma_{v,\infty}, Y, Z} \text{Tr}[\Sigma_{x,\infty}] \\
\text{s.t. } & \begin{bmatrix} \Sigma_{x,\infty}^- - \Sigma_{x,\infty} & \Sigma_{x,\infty}^- C^\top \\ C \Sigma_{x,\infty}^- & C \Sigma_{x,\infty}^- C^\top + \Sigma_{v,\infty} \end{bmatrix} \succeq 0 \\
& \begin{bmatrix} \hat{\Sigma}_w & Y \\ Y^\top & \Sigma_{w,\infty} \end{bmatrix} \succeq 0, \quad \begin{bmatrix} \hat{\Sigma}_v & Z \\ Z^\top & \Sigma_{v,\infty} \end{bmatrix} \succeq 0 \\
& \Sigma_{x,\infty}^- = A \Sigma_{x,\infty} A^\top + \Sigma_{w,\infty} \\
& \text{Tr}[\Sigma_{w,\infty} + \hat{\Sigma}_w - 2Y] \leq \theta_w^2 \\
& \text{Tr}[\Sigma_{v,\infty} + \hat{\Sigma}_v - 2Z] \leq \theta_v^2 \\
& \Sigma_{w,\infty} \succeq \lambda_{\min}(\hat{\Sigma}_w) I_{n_x}, \Sigma_{v,\infty} \succeq \lambda_{\min}(\hat{\Sigma}_v) I_{n_y} \\
& \Sigma_{x,\infty}^-, \Sigma_{x,\infty}, \Sigma_{w,\infty} \in \mathbb{S}_{++}^{n_x}, \Sigma_{v,\infty} \in \mathbb{S}_{++}^{n_y} \\
& Y \in \mathbb{R}^{n_x \times n_x}, Z \in \mathbb{R}^{n_y \times n_y}.
\end{aligned} \tag{13}$$

Algorithm 1 Time-Varying DRKF

Require: System matrices $\{A_t, C_t\}_{t=0}^{T-1}$, nominal means and covariances $(\hat{w}_t, \hat{v}_t, \hat{\Sigma}_{w,t}, \hat{\Sigma}_{v,t})$, prior state mean \hat{x}_0^- and covariance $\hat{\Sigma}_{x,0}^-$, ambiguity radii $(\theta_w, \theta_v, \theta_{x_0})$, horizon length T

- 1: Solve (4) to obtain $(\Sigma_{x,0}^{*}, \Sigma_{v,0}^{*})$ ▷ Offline stage
- 2: Compute DR gain K_0 via (8) and update the posterior covariance $\Sigma_{x,0}$ via (10)
- 3: **for** $t = 1, \dots, T-1$ **do**
- 4: Solve (7) to obtain $(\Sigma_{w,t-1}^{*}, \Sigma_{v,t}^{*}, \Sigma_{x,t}^{*}, \Sigma_{x,t})$
- 5: Compute DR gain K_t via (8)
- 6: **end for**
- 7: Set $\bar{x}_0^- = \hat{x}_0^-$ ▷ Online stage
- 8: **for** $t = 0, \dots, T-1$ **do**
- 9: Observe y_t
- 10: Update the state estimate \bar{x}_t via (9) using K_t
- 11: Predict the prior mean \bar{x}_{t+1}^- via (11)
- 12: **end for**

Algorithm 2 Steady-State DRKF

Require: System matrices (A, C) , nominal means and covariances $(\hat{w}, \hat{v}, \hat{\Sigma}_w, \hat{\Sigma}_v)$, prior state mean \hat{x}_0^- , ambiguity radii (θ_w, θ_v) ▷ Offline stage

- 1: Solve (13) to obtain $(\Sigma_{w,\infty}^{*}, \Sigma_{v,\infty}^{*}, \Sigma_{x,\infty}^{*}, \Sigma_{x,\infty}^{*})$
- 2: Compute the steady-state DR gain via (14)
- 3: Set $\bar{x}_0^- = \hat{x}_0^-$ ▷ Online stage
- 4: **for** $t = 0, 1, 2, \dots$ **do**
- 5: Observe y_t
- 6: Update the state estimate \bar{x}_t via (15) using K_∞^*
- 7: Predict the prior mean \bar{x}_{t+1}^- via (16)
- 8: **end for**

The optimal solution $\{\Sigma_{w,\infty}^{*}, \Sigma_{v,\infty}^{*}, \Sigma_{x,\infty}^{*}, \Sigma_{x,\infty}^{*}\}$ defines the least-favorable stationary covariances and yields the steady-state DR Kalman gain

$$K_\infty^* := \Sigma_{x,\infty}^{*} C^\top (C \Sigma_{x,\infty}^{*} C^\top + \Sigma_{v,\infty}^{*})^{-1}. \quad (14)$$

The resulting time-invariant estimator is

$$\bar{x}_t = \psi_\infty^*(\mathcal{Y}_t) := \bar{x}_t^- + K_\infty^*(y_t - C\bar{x}_t^- - \hat{v}), \quad (15)$$

with the prior update

$$\bar{x}_{t+1}^- = A\bar{x}_t + \hat{w}. \quad (16)$$

Compared with the finite-horizon DRKF, the steady-state filter (15) requires solving only a single stationary SDP offline. This makes it particularly suitable for real-time implementation. More importantly, it directly optimizes worst-case asymptotic performance, providing robustness to persistent disturbances and long-term distributional errors—an essential property for safety-critical systems with slow or unstable dynamics.

3.3 Algorithms and Complexity

We summarize the proposed DRKF methods for both the time-varying and steady-state settings. The two variants differ only in how the noise covariances (and hence the Kalman gains) are computed offline to ensure robustness against distributional ambiguity.

3.3.1 Time-Varying and Steady-State DRKF

As shown in Algorithm 1, the time-varying DRKF is implemented by solving the stage-wise SDP problems (4) and (5) offline over a horizon T . This yields the least-favorable noise covariances and the corresponding DR gains $\{K_t\}$. If the nominal covariances are known *a priori*, these gains can be fully precomputed.

Under the time-invariant assumptions of Section 3.2, the DRKF recursion may converge to a stationary solution. In this case, the offline stage reduces to solving the *single* stationary SDP (13), which yields the least-favorable noise covariances, the steady-state prior and posterior covariances, and the constant DR Kalman gain K_∞^* .

In both cases, the online stage performs only the standard KF measurement update and prediction, and thus has the same per-step computational complexity as the classical KF.

3.3.2 Discussion on Computational Complexity

The computational cost of the proposed DRKF methods is dominated by the *offline* SDP computations; the *online* recursion has the same per-step complexity as the classical KF.

In the time-varying case, each stage requires solving the SDP (7), whose decision variables include covariance blocks of size $n_x \times n_x$ and $n_y \times n_y$. This yields $\mathcal{O}(n_x^2 + n_y^2)$ free variables, with the largest linear matrix inequality (LMI) block of dimension $\mathcal{O}(n_x + n_y)$. Using standard interior-point methods [28], the per-stage complexity is $\tilde{\mathcal{O}}((n_x + n_y)^{3.5})$,⁷ and the total offline cost over a horizon T scales as $\tilde{\mathcal{O}}((n_x + n_y)^{3.5}T)$.

For comparison, the stage-wise DRKF of [17] and the DR-MMSE estimator of [18] also require solving a convex program at each stage. The former relies on joint state–measurement covariances of dimension $(n_x + n_y)$, leading to similar polynomial scaling but with larger LMI blocks and constants. Like our time-varying DRKF, these methods scale linearly with T , but they do not admit a steady-state formulation that reduces the offline computation to a *single* SDP.

Temporally coupled ambiguity sets, as in [21], model long-range dependence across the noise sequence at the cost of significantly higher complexity: all T stages are merged into a single horizon-level SDP whose size grows linearly with T , resulting in interior-point complexity of $\tilde{\mathcal{O}}(n_x^6 T^6)$. By contrast, our noise-centric formulation solves a *fixed-size* SDP at each stage, so the offline cost grows only linearly in T .

In the infinite-horizon setting, [21] characterizes the steady-state filter via a frequency-domain max-min problem over Toeplitz operators, producing a generally non-rational filter that requires spectral factorization and approximation for implementation. No finite-dimensional formulation is available. In contrast, our steady-state DRKF is obtained from a *single* stationary SDP of size $(n_x + n_y)$ with offline complexity $\tilde{\mathcal{O}}((n_x + n_y)^{3.5})$. It directly yields a constant gain K_∞^* and an online recursion matching the classical steady-state KF. Although this stage-wise ambiguity does not model temporal noise correlations, it preserves the separability of the Riccati recursion and keeps the DR filter tractable for real-time use.

⁷Here, $\tilde{\mathcal{O}}(\cdot)$ suppresses polylogarithmic factors.

4 Theoretical Analysis

Having established the DRKF formulations in both the finite- and infinite-horizon settings, we now analyze their fundamental theoretical properties. Our goal is to show that the DRKF retains key structural guarantees of the classical KF, such as stability and boundedness, while providing provable robustness under distributional uncertainty. In particular, we demonstrate that the DRKF covariance recursion remains spectrally bounded and that its steady-state solution inherits standard convergence properties of the classical filter.

4.1 Spectral Boundedness

We begin by quantifying how Wasserstein ambiguity sets constrain the least-favorable covariance matrices, and how these constraints propagate through the DRKF recursion in Theorem 1. This analysis shows that the DRKF operates within a uniformly bounded spectral envelope, a property that underpins its stability and distinguishes it from several existing robust formulations.

Our starting point is a well-known characterization of the (non-squared) Bures–Wasserstein distance.

Lemma 2. [29, Thm. 1] *Let $A, B \in \mathbb{S}_+^n$. The Bures–Wasserstein distance satisfies*

$$\mathcal{B}(A, B) = \min_{U \in O(n)} \|A^{1/2} - B^{1/2}U\|_F,$$

where $O(n)$ denotes the orthogonal group. The minimizer exists and is given by the orthogonal factor in the polar decomposition of $B^{1/2}A^{1/2}$.

This characterization enables sharp spectral bounds for matrices within a Bures–Wasserstein ball.

Proposition 1. *Fix $\hat{X} \in \mathbb{S}_+^n$. For any $X \in \mathbb{S}_+^n$ satisfying $\mathcal{B}(X, \hat{X}) \leq \theta$, the minimum and maximum eigenvalues of X are bounded as*

$$\underline{\lambda}(\hat{X}, \theta) \leq \lambda_{\min}(X) \leq \lambda_{\max}(X) \leq \bar{\lambda}(\hat{X}, \theta),$$

where

$$\begin{aligned} \underline{\lambda}(\hat{X}, \theta) &:= \left(\max \left\{ 0, \sqrt{\lambda_{\min}(\hat{X})} - \theta \right\} \right)^2, \\ \bar{\lambda}(\hat{X}, \theta) &:= \left(\sqrt{\lambda_{\max}(\hat{X})} + \theta \right)^2. \end{aligned}$$

The proof is provided in Appendix B.1. This result shows that a Bures–Wasserstein ball induces both upper and lower spectral bounds on feasible covariance matrices, defining an *eigenvalue tube* around the nominal covariance. This geometric perspective is essential: it rules out pathological behavior in which worst-case covariances can become arbitrarily inflated or collapse in directions that are inconsistent with the nominal statistics. As a result, the DRKF operates within a controlled spectral envelope under distributional perturbations allowed by the ambiguity sets. By contrast, KL-based ambiguity sets may admit least-favorable distributions with highly distorted or ill-conditioned covariance structure, leading to potentially pathological estimators [26].

We now translate these spectral bounds to the least-favorable noise covariances that enter the DRKF recursion.

Corollary 2. Let $\hat{\Sigma}_{v,t} \in \mathbb{S}_{++}^{n_y}$ and $\hat{\Sigma}_{w,t} \in \mathbb{S}_+^{n_x}$ denote the nominal noise covariances. For ambiguity radii $\theta_v, \theta_w, \theta_{x_0}$, define

$$\begin{aligned}\underline{\lambda}_{v,t} &:= \lambda_{\min}(\hat{\Sigma}_{v,t}), & \bar{\lambda}_{v,t} &:= \bar{\lambda}(\hat{\Sigma}_{v,t}, \theta_v), \\ \underline{\lambda}_{w,t} &:= \lambda_{\min}(\hat{\Sigma}_{w,t}), & \bar{\lambda}_{w,t} &:= \bar{\lambda}(\hat{\Sigma}_{w,t}, \theta_w), \\ \underline{\lambda}_{x,0} &:= \lambda_{\min}(\hat{\Sigma}_{x,0}^-), & \bar{\lambda}_{x,0} &:= \bar{\lambda}(\hat{\Sigma}_{x,0}^-, \theta_{x_0}).\end{aligned}\tag{17}$$

Then, the least-favorable covariances $\Sigma_{v,t}^*, \Sigma_{w,t}^*$ and $\Sigma_{x,0}^{-,*}$ obtained from (4)–(5) satisfy

$$\begin{aligned}\underline{\lambda}_{v,t} I_{n_y} &\preceq \Sigma_{v,t}^* \preceq \bar{\lambda}_{v,t} I_{n_y}, \\ \underline{\lambda}_{w,t} I_{n_x} &\preceq \Sigma_{w,t}^* \preceq \bar{\lambda}_{w,t} I_{n_x}, \\ \underline{\lambda}_{x,0} I_{n_x} &\preceq \Sigma_{x,0}^{-,*} \preceq \bar{\lambda}_{x,0} I_{n_x}.\end{aligned}$$

The proof is provided in Appendix B.2. In the time-invariant setting, the constants $\underline{\lambda}_w := \lambda_{\min}(\hat{\Sigma}_w)$, $\underline{\lambda}_v := \lambda_{\min}(\hat{\Sigma}_v)$, $\bar{\lambda}_w := \bar{\lambda}(\hat{\Sigma}_w, \theta_w)$, and $\bar{\lambda}_v := \bar{\lambda}(\hat{\Sigma}_v, \theta_v)$ are fixed. Thus, Corollary 2 ensures that the DRKF operates within a compact spectral envelope determined solely by the nominal statistics and the Wasserstein radii.

Theorem 2. Consider two classical KFs with noise covariances chosen according to the lower and upper bounds in (17). Let $(\underline{\Sigma}_{x,t}^-, \Sigma_{x,t}^-)$ and $(\bar{\Sigma}_{x,t}^-, \bar{\Sigma}_{x,t})$ denote their respective prior and posterior error covariances, with initial conditions $\underline{\Sigma}_{x,0}^- = \underline{\lambda}_{x,0} I_{n_x}$ and $\bar{\Sigma}_{x,0}^- = \bar{\lambda}_{x,0} I_{n_x}$. Then, for all $t \geq 0$, the DRKF covariances $(\Sigma_{x,t}^-, \Sigma_{x,t})$ satisfy

$$\underline{\Sigma}_{x,t}^- \preceq \Sigma_{x,t}^- \preceq \bar{\Sigma}_{x,t}^-,\quad \underline{\Sigma}_{x,t} \preceq \Sigma_{x,t} \preceq \bar{\Sigma}_{x,t}.$$

The proof is provided in Appendix B.3. Given the initial prior state covariance, the lower and upper bounds in Theorem 2 can be precomputed by running two standard KF recursions before solving the optimization problems (4) (for $t = 0$) and (5) (for $t > 0$).

This spectral boundedness is a direct consequence of our ambiguity set design, which models uncertainty separately for the process and measurement noise distributions. In contrast, previous DRKFs based on ambiguity sets centered on the joint prior-measurement distributions, as in [1], do not directly admit such precomputed spectral bounds. This highlights an additional advantage of our noise-centric construction, complementing the benefit noted in Remark 1.

4.2 Convergence

Having established the key theoretical properties of the least-favorable covariance matrices, we now derive conditions under which the DRKF admits a unique steady-state solution, and the sequence of time-varying gains converges to its steady-state value. Specifically, recall that the stationary DR Kalman gain K_∞^* is defined in (14). Our goal is to show that

$$\lim_{t \rightarrow \infty} K_t = K_\infty^*.$$

Under the standing assumptions, the time-varying SDP problems (4) and (5) admit optimal solutions (the feasible sets are nonempty and compact under the Bures–Wasserstein bounds), and therefore the sequence of DR Kalman gains $\{K_t\}$ is well defined. In the time-invariant setting, the steady-state SDP (13) is feasible (e.g., by choosing the nominal covariances), and below we show that the DR Riccati recursion converges to a unique fixed point characterized by this SDP.

The prior covariance recursion (12) can be equivalently expressed as

$$\Sigma_{x,t+1}^- = A((\Sigma_{x,t}^-)^{-1} + C^\top(\Sigma_{v,t}^*)^{-1}C)^{-1}A^\top + \Sigma_{w,t}^*, \quad (18)$$

with $\Sigma_{x,0}^- = \Sigma_{x,0}^{-,*}$. If $\hat{\Sigma}_{x,0}^- \succ 0$, then $\Sigma_{x,0}^- \succ 0$ and the recursion is well defined.⁸ This motivates the following definition of the *DR Riccati mapping*:

$$r_{\mathbb{D}}(\Sigma_{x,t}^-) := A((\Sigma_{x,t}^-)^{-1} + C^\top(\Sigma_{v,t}^*)^{-1}C)^{-1}A^\top + \Sigma_{w,t}^*. \quad (19)$$

Under Assumption 2, the problem data of the stage-wise SDP are time-invariant. Accordingly, the sequence $\{(\Sigma_{w,t}^*, \Sigma_{v,t}^*)\}$ is generated by repeatedly applying the same SDP template along the state covariance trajectory. Observing the structural similarity with Riccati equations arising in robust and risk-sensitive filtering (e.g., [5, 30]), we pursue contraction-based analysis in this subsection.

We begin by imposing the standard observability assumption.⁹

Assumption 3. *The pair (A, C) is observable.*

To establish strict contraction under the observability assumption, we employ a downsampled (lifted) representation of the DR Riccati recursion, since the one-step mapping may fail to be contractive due to rank-deficient measurement operators, whereas observability guarantees full column rank of the lifted observability matrix.

Fix $N \in \mathbb{N}$ and consider the system (1) under the least-favorable distributions. Define the downsampled state as $x_t^d := x_{tN}$. Downsampling yields an N -block lifted model with block-diagonal uncertainty structure, enabling a contraction argument similar to [31, 32]. Let $\mathbf{w}_t^N := [w_{tN+N-1}^\top, \dots, w_{tN}^\top]^\top$, and $\mathbf{v}_t^N := [v_{tN+N-1}^\top, \dots, v_{tN}^\top]^\top$ denote the stacked process and measurement noise vectors, with means $\mathbf{1}_N \otimes \hat{w}$ and $\mathbf{1}_N \otimes \hat{v}$, and covariances $\Sigma_{w,t}^{N,*} := \text{blkdiag}(\Sigma_{w,tN+N-1}^*, \dots, \Sigma_{w,tN}^*)$ and $\Sigma_{v,t}^{N,*} := \text{blkdiag}(\Sigma_{v,tN+N-1}^*, \dots, \Sigma_{v,tN}^*)$, respectively. The downsampled dynamics then take the form

$$\begin{aligned} x_{t+1}^d &= A^N x_t^d + \mathcal{R}_N \mathbf{w}_t^N \\ \mathbf{y}_t^N &= \mathcal{O}_N x_t^d + \mathcal{H}_N \mathbf{w}_t^N + \mathbf{v}_t^N, \end{aligned}$$

where $\mathbf{y}_t^N := [y_{tN+N-1}^\top, \dots, y_{tN}^\top]^\top$ is the stacked observation vector, while the block reachability and observability matrices are defined as

$$\mathcal{R}_N := [I_{n_x}, A, \dots, A^{N-1}] \quad (20)$$

$$\mathcal{O}_N := [(CA^{N-1})^\top, \dots, (CA)^\top, C^\top]^\top. \quad (21)$$

The block Toeplitz matrix $\mathcal{H}_N \in \mathbb{R}^{Nn_y \times Nn_x}$ captures the propagation of process noise into future outputs and is defined elementwise by $[\mathcal{H}_N]_{ij} = CA^{j-i-1}$, $j > i$, and zero otherwise, for $i, j = 1, \dots, N$. Let $\mathbf{u}_t^N := \mathcal{H}_N \mathbf{w}_t^N + \mathbf{v}_t^N$. Its covariance is given by $\Sigma_{u,t}^N = \mathcal{H}_N \Sigma_{w,t}^{N,*} \mathcal{H}_N^\top + \Sigma_{v,t}^{N,*}$. Adopting the procedure in [33] and denoting the downsampled prior covariance matrix by $\Sigma_{x,t}^{-,d} := \Sigma_{x,tN}^-$, the DR Riccati recursion associated with the downsampled model becomes

$$\Sigma_{x,t+1}^{-,d} = r_{\mathbb{D},t}^d(\Sigma_{x,t}^{-,d}), \quad (22)$$

⁸If $\hat{\Sigma}_{x,0}^- \succeq 0$, the uniform bound $\Sigma_{w,t}^* \succeq \underline{\lambda}_w I$ ensures that $\Sigma_{x,1}^- \in \mathbb{S}_{++}^{n_x}$, so the information-form recursion is well defined from time $t = 1$ onward.

⁹Since $\hat{\Sigma}_w \succ 0$ and $\Sigma_{w,t}^* \succeq \underline{\lambda}_w I$, the process noise covariance is uniformly positive definite; hence no additional controllability assumption is required.

where

$$r_{\mathbb{D},t}^d(\Sigma_{x,t}^{-,d}) = \alpha_{N,t} \left((\Sigma_{x,t}^{-,d})^{-1} + \Omega_{N,t} \right)^{-1} (\alpha_{N,t})^\top + W_{N,t}, \quad (23)$$

with

$$\begin{aligned} \alpha_{N,t} &:= A^N - \mathcal{R}_N \mathcal{G}_{N,t} \mathcal{O}_N \\ \Omega_{N,t} &:= \mathcal{O}_N^\top (\Sigma_{u,t}^N)^{-1} \mathcal{O}_N \\ W_{N,t} &:= \mathcal{R}_N \mathcal{Q}_{N,t} \mathcal{R}_N^\top \\ \mathcal{Q}_{N,t} &:= \Sigma_{w,t}^{N,*} - \Sigma_{w,t}^{N,*} \mathcal{H}_N^\top (\Sigma_{u,t}^N)^{-1} \mathcal{H}_N \Sigma_{w,t}^{N,*} \\ \mathcal{G}_{N,t} &:= \Sigma_{w,t}^{N,*} \mathcal{H}_N^\top (\Sigma_{u,t}^N)^{-1}. \end{aligned}$$

Under Assumption 2, the one-step DR Riccati update is time-invariant, and the corresponding downsampled mapping $r_{\mathbb{D},t}^d$ coincides with the N -fold iterate $r_{\mathbb{D}}^N$ of a single Riccati operator $r_{\mathbb{D}}$. We therefore analyze contraction properties of the DR Riccati recursion through this lifted representation, via a downsampling contraction argument in the spirit of [32].

We first establish basic structural properties of $\Omega_{N,t}$ and $W_{N,t}$, which are required for the contraction analysis.

Lemma 3. *Suppose Assumptions 1 to 3 hold. Then, $W_{N,t} \in \mathbb{S}_{++}^{n_x}$ for any $N \geq 1$ and $\Omega_{N,t} \in \mathbb{S}_{++}^{n_x}$ for any $N \geq n_x$.*

The proof is provided in Appendix C.1.

Using the above properties, we establish contraction of the (downsampled) DR Riccati mapping with respect to Thompson's part metric, defined as follows: for $P, Q \in \mathbb{S}_{++}^{n_x}$,

$$d_T(P, Q) := \log \left(\max \{ \lambda_{\max}(P^{-1}Q), \lambda_{\max}(Q^{-1}P) \} \right).$$

This metric is invariant under congruence transformations and is well suited for analyzing Riccati-type mappings.

Lemma 4. *Suppose Assumptions 1 to 3 hold and let $N \geq n_x$, so that \mathcal{O}_N has full column rank. Then, for any $t \geq 0$, the downsampled DR Riccati mapping $r_{\mathbb{D},t}^d$ (23) is strictly contractive on $\mathbb{S}_{++}^{n_x}$ with respect to d_T : there exists $\xi_{N,t} \in (0, 1)$ such that*

$$d_T(r_{\mathbb{D},t}^d(P), r_{\mathbb{D},t}^d(Q)) \leq \xi_{N,t} d_T(P, Q), \quad \forall P, Q \in \mathbb{S}_{++}^{n_x}.$$

Moreover, the contraction factor satisfies the bound

$$\xi_{N,t} \leq \left(\frac{\sqrt{\|M_{N,t}\|_2}}{1 + \sqrt{1 + \|M_{N,t}\|_2}} \right)^2, \quad (24)$$

where $M_{N,t} := \Omega_{N,t}^{-1/2} \alpha_{N,t}^\top W_{N,t}^{-1} \alpha_{N,t} \Omega_{N,t}^{-1/2}$.

This follows from [34, Thm. 5.3] together with Lemma 3.

We next show that the contraction factor can be bounded *uniformly* over time by exploiting the spectral envelope induced by Wasserstein ambiguity.

Proposition 2. Suppose that Assumptions 1 to 3 hold. Fix $N \geq n_x$ and define

$$\begin{aligned} \kappa_N(\theta_v, \theta_w) &:= \frac{\bar{\lambda}(\hat{\Sigma}_v, \theta_v) + \bar{\lambda}(\hat{\Sigma}_w, \theta_w) \|\mathcal{H}_N\|_2^2}{\sigma_{\min}(\mathcal{O}_N)^2} \\ &\quad \times \left(\|A^N\|_2 + \frac{\bar{\lambda}(\hat{\Sigma}_w, \theta_w) \|\mathcal{H}_N\|_2 \|\mathcal{R}_N\|_2 \|\mathcal{O}_N\|_2}{\lambda_{\min}(\hat{\Sigma}_v)} \right)^2 \left(\frac{1}{\lambda_{\min}(\hat{\Sigma}_w)} + \frac{\|\mathcal{H}_N\|_2^2}{\lambda_{\min}(\hat{\Sigma}_v)} \right), \end{aligned} \quad (25)$$

where $\bar{\lambda}(\cdot, \cdot)$ is defined as in Proposition 1. Then, for all $t \geq 0$, the contraction factor in (24) satisfies

$$\xi_{N,t} \leq \bar{\xi}_N(\theta_v, \theta_w) := \left(\frac{\sqrt{\kappa_N(\theta_v, \theta_w)}}{1 + \sqrt{1 + \kappa_N(\theta_v, \theta_w)}} \right)^2 \in (0, 1).$$

In particular, for any prescribed $\rho \in (0, 1)$, any radii (θ_v, θ_w) satisfying

$$\kappa_N(\theta_v, \theta_w) \leq \frac{4\rho}{(1 - \rho)^2} \quad (26)$$

ensure $\xi_{N,t} \leq \rho$ for all t .

The proof is provided in Appendix C.2.

Combining the pointwise contraction in Lemma 4 with the uniform bound in Proposition 2 yields convergence of the DR Riccati recursion.

Theorem 3. Suppose Assumptions 1 to 3 hold and let $N \geq n_x$. Then, for any $t \geq 0$, the downsampled DR Riccati mapping $r_{\mathbb{D},t}^d$ is strictly contractive on $\mathbb{S}_{++}^{n_x}$ with respect to Thompson's part metric, with contraction factor $\xi_{N,t}$ satisfying

$$\xi_{N,t} \leq \bar{\xi}_N(\theta_v, \theta_w) < 1 \quad \forall t \geq 0.$$

Consequently, the full DR Riccati recursion (18) converges to a unique fixed point $\Sigma_{x,\infty}^- \succ 0$, and the associated DR Kalman gain K_t converges.

The proof is provided in Appendix C.3.

As a consequence of Theorem 3, the steady-state solution can be obtained by solving the single stationary SDP (13) offline, rather than via online Riccati iterations.

Corollary 3. Under the assumptions of Theorem 3, the steady-state covariance matrices $(\Sigma_{x,\infty}^-, \Sigma_{x,\infty}^*)$, together with the least-favorable noise covariances $\Sigma_{w,\infty}^*$ and $\Sigma_{v,\infty}^*$, solve the stationary SDP (13). Consequently, $K_\infty^* = \lim_{t \rightarrow \infty} K_t$.

The proof can be found in Appendix C.4.

Under Assumption 3, the Riccati recursions of the standard KFs in Theorem 2 converge. Taking limits in the matrix inequalities $A \preceq B$ (in the sense of the Loewner partial order) appearing in Theorem 2, and using that the positive semidefinite cone is closed, yields the following steady-state bounds.

Corollary 4. Under the assumptions of Theorem 3, the steady-state prior and posterior error covariances $\Sigma_{x,\infty}^-$ and $\Sigma_{x,\infty}$ satisfy

$$\underline{\Sigma}_{x,\infty}^- \preceq \Sigma_{x,\infty}^- \preceq \bar{\Sigma}_{x,\infty}^-, \quad \underline{\Sigma}_{x,\infty} \preceq \Sigma_{x,\infty} \preceq \bar{\Sigma}_{x,\infty},$$

where $\underline{\Sigma}_{x,\infty}^- := \lim_{t \rightarrow \infty} \underline{\Sigma}_{x,t}^-$ and $\bar{\Sigma}_{x,\infty}^- := \lim_{t \rightarrow \infty} \bar{\Sigma}_{x,t}^-$ (and similarly for $\underline{\Sigma}_{x,\infty}$, $\bar{\Sigma}_{x,\infty}$) are the unique steady-state limits of the lower- and upper-bound KF recursions in Theorem 2.

Remark 4. Since $\bar{\lambda}(\hat{X}, \theta)$ is nondecreasing in θ for $\theta \geq 0$, the bound $\kappa_N(\theta_v, \theta_w)$ in (25) is monotone in both ambiguity radii. Consequently, a practical tuning procedure for (θ_v, θ_w) consists of enforcing the rate constraint (26) using one of the following strategies: (i) fix θ_v and determine the largest admissible θ_w ; (ii) fix θ_w and determine the largest admissible θ_v ; or (iii) restrict (θ_v, θ_w) to a one-dimensional curve (e.g., $\theta_w = \gamma\theta_v$ for some $\gamma > 0$) and select the maximal radii satisfying (26). These procedures allow one to balance robustness and convergence speed in a transparent and computationally tractable manner.

4.3 Stability

A key property of the classical Kalman filter is the stability of its steady-state estimation error dynamics: under detectability of (A, C) and positive definite process noise, the closed-loop error matrix $(I - KC)A$ is Schur stable, ensuring bounded error covariance and asymptotic convergence of the estimation error in the unbiased case.

In the distributionally robust setting, however, the estimator is designed against least-favorable noise distributions within ambiguity sets. It is thus nontrivial whether the resulting DRKF, whose steady-state gain is characterized by the minimax design in Theorem 3, preserves the stability guarantees of the classical KF. The following result shows that, despite the adversarial nature of the noise model, the steady-state DRKF remains asymptotically stable in the same sense as the classical KF.

Theorem 4. Suppose Assumptions 1 to 3 hold. Let $(\Sigma_{x,\infty}^{-*}, \Sigma_{x,\infty}^*)$ and $(\Sigma_{w,\infty}^*, \Sigma_{v,\infty}^*)$ denote the steady-state DRKF covariances, and let K_∞^* be the corresponding steady-state DR Kalman gain. Define the closed-loop error matrix $F_\infty := (I - K_\infty^* C)A$. Then, F_∞ is Schur stable, and the posterior estimation error $e_t := x_t - \bar{x}_t$ evolves according to

$$e_t = F_\infty e_{t-1} + (I - K_\infty^* C)(w_{t-1} - \hat{w}) - K_\infty^*(v_t - \hat{v}).$$

Consequently, under the least-favorable noise distributions, the estimation error is mean-square stable with

$$\sup_{t \geq 0} \mathbb{E}[\|e_t\|^2] < \infty, \quad \text{and} \quad \lim_{t \rightarrow \infty} \text{cov}(e_t) = \Sigma_{x,\infty}^*.$$

The proof is provided in Appendix D.1.

While Theorem 4 establishes mean-square stability, it does not by itself characterize the behavior of the estimation-error mean under model mismatch. In practice, the true noise processes may have means that differ from the nominal values used by the filter, leading to a steady-state bias. The following corollary characterizes this bias under the true noise distributions.

Corollary 5. Under the assumptions of Theorem 4, consider running the steady-state DRKF with gain K_∞^* on a system whose noise processes have constant (true) means $\mathbb{E}[w_t] = \mu_w$ and $\mathbb{E}[v_t] = \mu_v$ for all t , with finite first moments. Let $m_t := \mathbb{E}[e_t]$ denote the posterior error mean under the true noise distributions. Then, $m_t = F_\infty m_{t-1} + (I - K_\infty^* C)(\mu_w - \hat{w}) - K_\infty^*(\mu_v - \hat{v})$, and hence

$$\lim_{t \rightarrow \infty} m_t = (I - F_\infty)^{-1}((I - K_\infty^* C)(\mu_w - \hat{w}) - K_\infty^*(\mu_v - \hat{v})).$$

In particular, if the nominal noise means used by the filter coincide with the true noise means ($\hat{w} = \mu_w$ and $\hat{v} = \mu_v$), then $\mathbb{E}[e_t] \rightarrow 0$.

The proof is provided in Appendix D.2.

As shown in Lemma 1, mean shifts are suboptimal for the adversary under Wasserstein ambiguity at the design stage, so the least-favorable noise distributions preserve the nominal means. Therefore, when the nominal noise means used by the filter coincide with the true noise means, the steady-state DRKF is unbiased in operation. When this condition is violated, a constant steady-state bias appears, exactly as characterized in Corollary 5.

4.4 Optimality

Having established convergence and stability of the proposed DRKF, we now address its performance optimality. In the presence of distributional uncertainty, a natural question is whether one can design a causal estimator that outperforms the DRKF in terms of worst-case estimation accuracy.

In this subsection, we show that this is not possible asymptotically: among all causal estimators, the steady-state DRKF minimizes the worst-case one-step conditional mean-square error in the limit, as well as its long-run time average.

Theorem 5. *Suppose Assumptions 1 to 3 hold. Let $\Sigma_{x,\infty}^{-,*} \in \mathbb{S}_{++}^{n_x}$ denote the unique fixed point of the DR Riccati map $r_{\mathbb{D}}$ and let $\Sigma_{x,\infty}^*$ be the corresponding steady-state posterior error covariance. Then, for any causal state estimator sequence $\{\psi_t\}_{t \geq 0}$ with $\psi_t \in \mathcal{F}_t$, the following inequalities hold almost surely with respect to $\sigma(\mathcal{Y}_{t-1})$:*

$$\liminf_{t \rightarrow \infty} \sup_{\mathbb{P}_{e,t} \in \mathbb{D}_{e,t}} J_t(\psi_t, \mathbb{P}_{e,t}) \geq \text{Tr}[\Sigma_{x,\infty}^*], \quad (27)$$

$$\liminf_{T \rightarrow \infty} \frac{1}{T} \sum_{t=0}^{T-1} \sup_{\mathbb{P}_{e,t} \in \mathbb{D}_{e,t}} J_t(\psi_t, \mathbb{P}_{e,t}) \geq \text{Tr}[\Sigma_{x,\infty}^*]. \quad (28)$$

Moreover, the steady-state DRKF ψ_∞ with gain K_∞^* achieves these bounds with equality:

$$\lim_{t \rightarrow \infty} \sup_{\mathbb{P}_{e,t} \in \mathbb{D}_{e,t}} J_t(\psi_\infty, \mathbb{P}_{e,t}) = \text{Tr}[\Sigma_{x,\infty}^*], \quad (29)$$

$$\lim_{T \rightarrow \infty} \frac{1}{T} \sum_{t=0}^{T-1} \sup_{\mathbb{P}_{e,t} \in \mathbb{D}_{e,t}} J_t(\psi_\infty, \mathbb{P}_{e,t}) = \text{Tr}[\Sigma_{x,\infty}^*]. \quad (30)$$

Hence, the steady-state DRKF is asymptotically minimax-optimal with respect to the worst-case one-step and long-run average MSE.

The proof of is provided in Appendix D.3. This result shows that the steady-state DRKF attains the smallest possible worst-case asymptotic MSE among all causal estimators, thereby extending the fundamental optimality of the classical KF to the DR setting. Importantly, the theorem concerns *asymptotic* performance: establishing finite-horizon minimax optimality under stage-wise ambiguity leads to a substantially more intricate dynamic game and is beyond the scope of this work.

Remark 5. *When $\theta_v = \theta_w = 0$, the ambiguity sets reduce to the nominal noise distributions. In this case, the least-favorable covariances coincide with the nominal ones, and the DRKF reduces exactly to the classical KF. Thus, Theorem 5 is consistent with the classical KF optimality and recovers it as a special case in the asymptotic regime.*

5 Experiments

We evaluate the proposed DRKFs through numerical experiments that assess estimation accuracy, closed-loop performance, and computational efficiency, and that empirically validate the theoretical

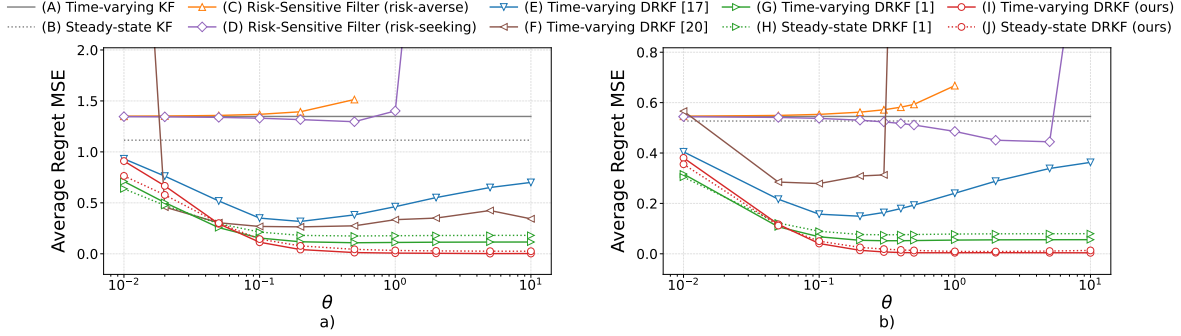


Figure 1: Effect of θ on the average regret MSE under a) Gaussian and b) U-Quadratic noise distributions, averaged over 20 simulation runs.

results in Section 4.¹⁰

5.1 Comparison of Robust State Estimators

We begin by comparing the proposed time-varying and steady-state DRKFs with the following baseline estimators:

- (A) Standard time-varying KF
- (B) Steady-state KF
- (C) Risk-sensitive filter (risk-averse) [5, 30, 32, 33]
- (D) Risk-sensitive filter (risk-seeking) [5, 30, 32, 33]
- (E) DRKF with joint Wasserstein ambiguity on (x_t, y_t) [17]
- (F) DRKF with bicausal Wasserstein ambiguity [20]¹¹
- (G) Time-varying DRKF with Wasserstein ambiguity on the prior state and measurement noise [1, Thm. 1]
- (H) Time-invariant version of (G) with stationary nominals [1, Sect. 4]
- (I) **Time-varying DRKF (ours)** [Algorithm 1]
- (J) **Steady-state DRKF (ours)** [Algorithm 2]

We use the same symbol θ to denote the robustness parameter across all methods, although its interpretation differs. For risk-sensitive filters (C) and (D), θ is the risk parameter (with opposite signs for risk-averse/seeking variants), chosen within the stability range [33]. For Wasserstein-based methods, θ denotes the ambiguity radius. For (G) and (H), we set $\theta_{x_0} = \theta_v = \theta$. In our proposed formulations, we set $\theta_{x_0} = \theta_w = \theta_v = \theta$ for (I), and $\theta_w = \theta_v = \theta$ for (J). To ensure fairness, we sweep each method over its admissible range of θ and report performance at the best tuned value.¹²

¹⁰All experiments were performed on a laptop equipped with an Intel Core Ultra 7 155H @ 3.80 GHz and 32 GB of RAM. Source code is available at <https://github.com/jangminhyuk/DRKF2025>.

¹¹Following [20], we cap the number of internal iterations at 20.

¹²In practice, DRKF radii θ can be selected from data, following standard approaches in the DRO literature, such as cross-validation or bootstrapping (e.g., [25, 35]).

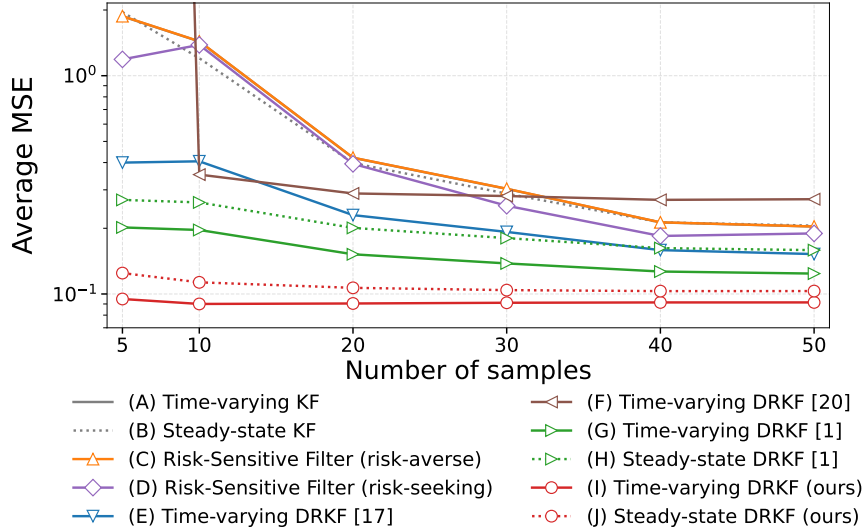


Figure 2: Effect of the number of samples used to construct the nominal distributions on the average MSE under Gaussian noise, averaged over 10 runs.

5.1.1 Estimation Accuracy

We first consider a linear time-invariant system, subject to inaccuracies in both the process and measurement noise distributions:

$$A = \begin{bmatrix} 1 & 0.2 & 0 & 0 \\ 0 & 0.2 & 0.2 & 0 \\ 0 & 0 & 0.2 & 0.2 \\ 0 & 0 & 0 & -1 \end{bmatrix}, \quad C = \begin{bmatrix} 1 & 0 & 0 & 0 \\ 0 & 0 & 1 & 0 \end{bmatrix}.$$

We test two noise models: (i) Gaussian, with $x_0 \sim \mathcal{N}(0, 0.01I_4)$, $w_t \sim \mathcal{N}(0, 0.01I_4)$, $v_t \sim \mathcal{N}(0, 0.01I_2)$, and (ii) U-Quadratic, with $x_0 \sim \mathcal{UQ}([-0.1, 0.1]^4)$, $w_t \sim \mathcal{UQ}([-0.1, 0.1]^4)$, $v_t \sim \mathcal{UQ}([-0.1, 0.1]^2)$. Nominal covariances are learned from only 10 measurement samples using the expectation-maximization (EM) method in [20], creating a significant mismatch between nominal and true noise statistics. The estimation horizon is $T = 50$.

Fig. 1 shows the effect of $\theta \in [10^{-2}, 10^1]$ on the average regret MSE under both noise models, averaged over 20 runs. The regret MSE is defined as the difference between the filter's MSE and that of the KF using the *true* noise distributions. The results show that both proposed DRKFs consistently achieve the lowest tuned regret and remain competitive across a wide range of θ . In particular, (I) achieves performance closest to the optimal estimator under both poorly estimated Gaussian and non-Gaussian noise.

In contrast, the BCOT-based DRKF (F) exhibits numerical instability and discontinuous performance across θ , even when increasing the internal iteration limit to 50. The risk-sensitive filters (C) and (D) become overly conservative for large θ , leading to degraded accuracy.

Fig. 2 further examines performance as a function of the number of samples used to estimate the nominal noise statistics.¹³ Across all sample sizes, the proposed DRKFs achieve the lowest MSE, with particularly clear advantages in the low-data regime.

¹³Each filter is optimally tuned over $\theta \in [10^{-2}, 10^1]$, and we vary the number of input-output samples used in the EM procedure so that small sample sizes correspond to less accurate nominal distributions.

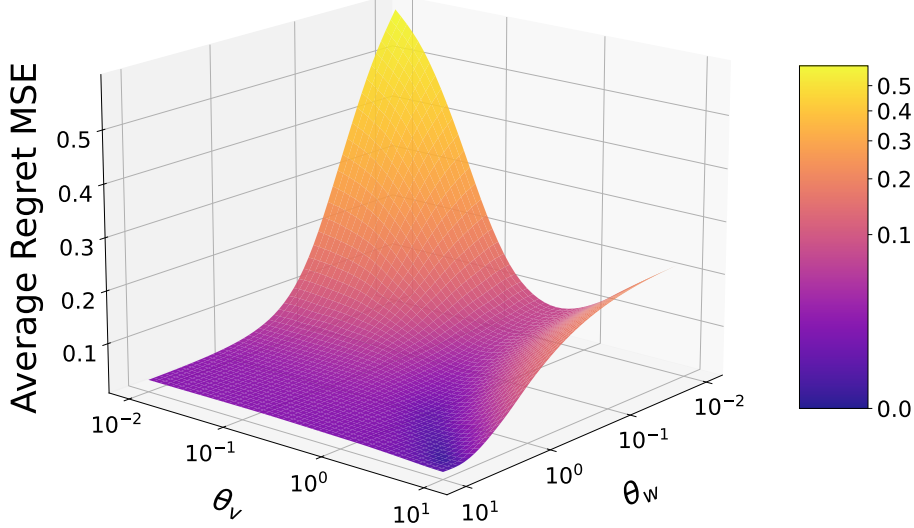


Figure 3: Average regret MSE of the proposed steady-state DRKF under Gaussian noise, as a function of θ_w and θ_v , averaged over 100 runs.

— (A) Time-varying KF ▲ (C) Risk-Sensitive Filter (risk-averse) ▽ (E) Time-varying DRKF [17] ▷ (G) Time-varying DRKF [1] ○ (I) Time-varying DRKF (ours)
 (B) Steady-state KF △ (D) Risk-Sensitive Filter (risk-seeking) △ (F) Time-varying DRKF [20] ▷ (H) Steady-state DRKF [1] ⋮ (J) Steady-state DRKF (ours)

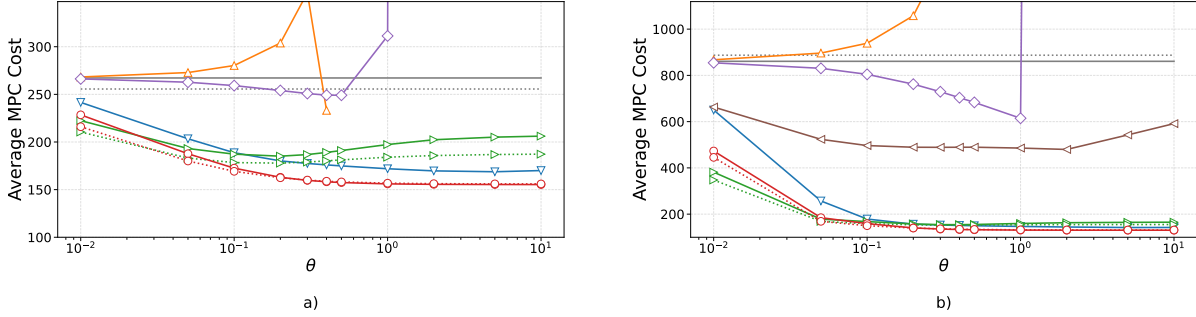


Figure 4: Effect of θ on the average MPC cost under a) Gaussian and b) nonzero-mean U-Quadratic noise, averaged over 20 simulation runs.

Table 1: Mean and standard deviation of the acceleration-command magnitude $\|u_t\|_2$ for each filter, averaged over 200 simulations.

	(A)	(B)	(E)	(F)	(G)	(H)	(I)	(J)
$\ u_t\ _2$	5.69 (7.44)	5.91 (7.70)	3.29 (1.93)	2.70 (1.78)	3.37 (2.02)	3.30 (1.99)	2.18 (1.63)	2.20 (1.64)

Fig. 3 illustrates the sensitivity of the steady-state DRKF to the ambiguity radii (θ_w, θ_v) . Insufficient robustness (small radii) leads to large regret, while overly large radii induce excessive conservatism, highlighting the need to balance θ_w and θ_v .

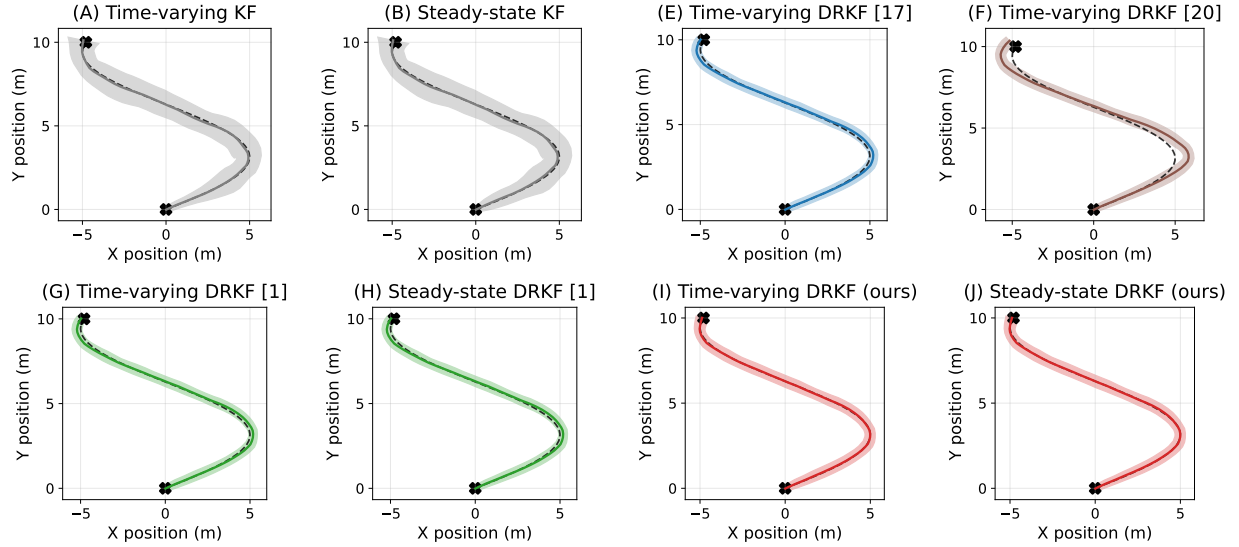


Figure 5: 2D trajectories averaged over 200 simulations. Each filter uses its optimal $\theta \in [10^{-2}, 10^1]$ minimizing the MPC cost. The dashed black line is the desired trajectory; colored curves show the mean, and shaded tubes indicate ± 1 standard deviation.

Table 2: Average offline computation time of the steady-state DRKF as a function of $n_x = n_y = n$ (10 runs).

n	5	10	15	20	25	30	35	40
Time (s)	0.0600	0.1794	0.4736	1.2414	2.2905	4.8900	8.3890	12.4232

5.1.2 Trajectory Tracking Task

We next evaluate closed-loop performance on a 2D trajectory-tracking task, following the setup in [1, Sect. 5.2]:

$$x_{t+1} = \begin{bmatrix} I_2 & \Delta t I_2 \\ \mathbf{0}_{2 \times 2} & I_2 \end{bmatrix} x_t + \begin{bmatrix} 0.5(\Delta t)^2 I_2 \\ \Delta t I_2 \end{bmatrix} u_t + w_t$$

$$y_t = [I_2 \quad \mathbf{0}_{2 \times 2}] x_t + v_t,$$

where $\Delta t = 0.2$ s. The state $x_t = [p_t^x, p_t^y, v_t^x, v_t^y]^\top$ collects the planar position and velocity, and the control input $u_t = [a_t^x, a_t^y]^\top$ represents acceleration commands. All methods use the same observer-based MPC controller, with the current state estimate \bar{x}_t provided by each filter. The controller solves a finite-horizon tracking problem with horizon 10 and weights $Q = \text{diag}([10, 10, 1, 1])$ and $R = 0.1I_2$, where Q penalizes tracking error and R penalizes control effort. The first control input u_t is applied, and the optimization is repeated at the next step using \bar{x}_{t+1} .

The true noise distributions are $x_0 \sim \mathcal{N}(0, 0.02I_4)$, $w_t \sim \mathcal{N}(0, 0.02I_4)$, and $v_t \sim \mathcal{N}(0, 0.02I_2)$, simulated over 10 s. For the nominal distributions, we fit an EM model using only 1 s of input-output data, yielding noticeably inaccurate nominal statistics and reflecting the practical challenge of estimating noise models from limited observations.

Fig. 4 shows the effect of θ on the average MPC cost, defined as the closed-loop quadratic sum of tracking error and input energy weighted by Q and R . Consistent with Section 5.1.1, both our

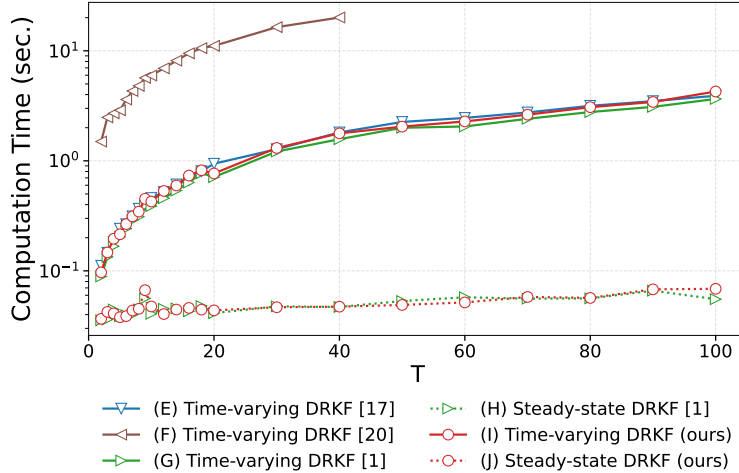


Figure 6: Average offline computation time as a function of the horizon length T for $n_x = 4$, $n_y = 2$, averaged over 10 runs.

time-varying and steady-state DRKFs achieve the lowest cost when optimally tuned, even in the presence of non-Gaussian disturbances and nonzero-mean noise.

Fig. 5 displays the mean trajectories and uncertainty envelopes obtained with the best-tuned radius $\theta \in [10^{-2}, 10^1]$ for each filter. The standard KFs (A) and (B) produce wider uncertainty tubes, indicating higher estimation variance. The BCOT-based DRKF (F) reduces dispersion but introduces greater bias, especially during sharp turns. Other DRKFs—(E), (G), and (H)—achieve improved tracking, while the proposed time-varying and steady-state DRKFs exhibit the lowest dispersion and bias.

Although mean trajectories are similar across DRKFs, control effort differs substantially. As shown in Table 1, the proposed DRKFs require the lowest average control energy among all methods.

5.1.3 Computation Time

Fig. 6 compares the offline computation time of (E)–(J) as a function of the horizon length T .¹⁴ Time-varying DRKFs exhibit linear growth in offline computation time with respect to T , with (F) being particularly expensive. In contrast, the steady-state DRKFs (H) and (J) maintain constant runtime, as they require solving only a single SDP offline. This demonstrates the scalability of the proposed steady-state DRKF for long-horizon applications.

Finally, Table 2 evaluates scalability with respect to the system dimension. For each n , we generate a random system with $n_x = n_y = n$ and measure the offline computation time. Even at $n = 40$, the total runtime remains under 13 seconds, confirming the practical efficiency of the steady-state DRKF for moderately sized systems.

5.2 Validation of Theoretical Properties

5.2.1 Covariance Sandwich Property

We illustrate the covariance sandwich property of Theorem 2 using a 2D example with

$$A = 0.95 \begin{bmatrix} \cos(\pi/8) & -\sin(\pi/8) \\ \sin(\pi/8) & \cos(\pi/8) \end{bmatrix}, \quad C = \begin{bmatrix} 1.0 & 0.1 \\ 0.1 & 1.0 \end{bmatrix},$$

¹⁴We use the same setup as in Section 5.1.1 with $\theta = 1.0$ and Gaussian noise.

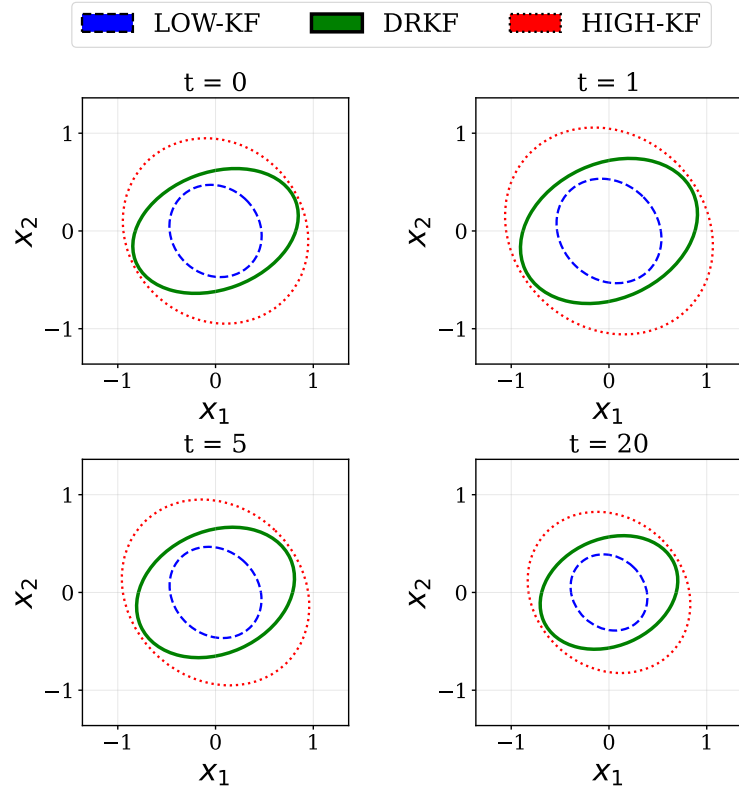


Figure 7: 95% confidence ellipses of the posterior covariances for LOW-KF, DRKF, and HIGH-KF at $t \in \{0, 1, 5, 20\}$.

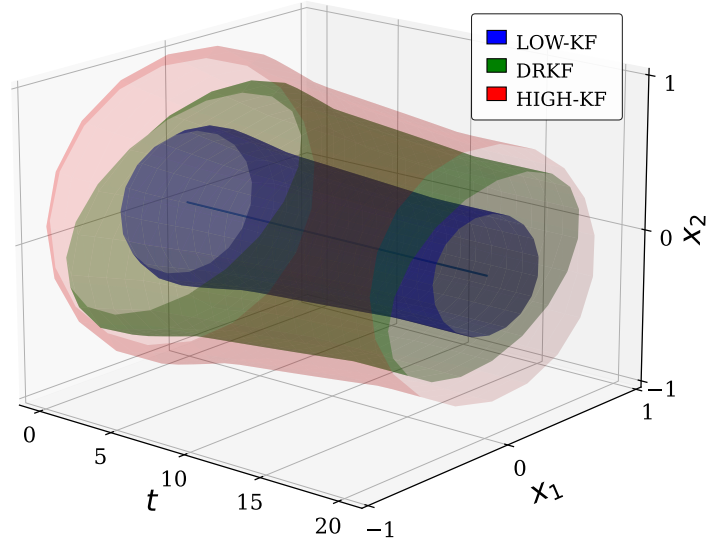


Figure 8: Three-dimensional tube visualization obtained by stacking the 95% ellipses of the posterior covariances of LOW-KF, DRKF, and HIGH-KF for $t = 0, \dots, 20$.

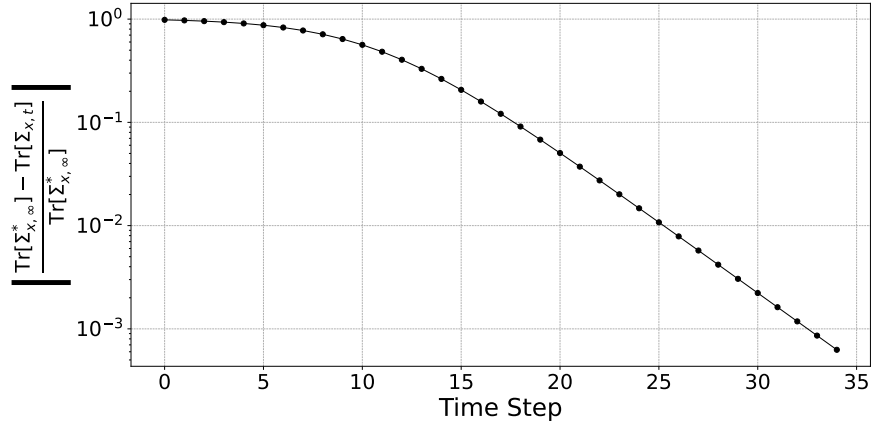


Figure 9: Relative difference between $\text{Tr}[\Sigma_{x,t}]$ and $\text{Tr}[\Sigma_{x,\infty}^*]$.

horizon $T = 20$, and ambiguity radii $\theta_w = \theta_v = \theta_{x_0} = 0.1$. The initial prior covariance is $\Sigma_{x,0}^- = \begin{bmatrix} 0.2 & 0.05 \\ 0.05 & 0.1 \end{bmatrix}$. We use time-varying nominal covariances of the form $\hat{\Sigma}_{w,t} = a_t \hat{\Sigma}_w$, $\hat{\Sigma}_{v,t} = a_t \hat{\Sigma}_v$, constructed by scaling the base matrices

$$\hat{\Sigma}_w = \begin{bmatrix} 0.3 & 0.1 \\ 0.1 & 0.2 \end{bmatrix}, \quad \hat{\Sigma}_v = \begin{bmatrix} 0.15 & 0.05 \\ 0.05 & 0.1 \end{bmatrix},$$

with piecewise-linear factors a_t :

$$a_t = \begin{cases} 1 - 0.06t, & 0 \leq t \leq 5, \\ 0.7 - 0.02(t - 5), & 5 < t \leq 15, \\ 0.5, & t > 15. \end{cases}$$

These covariances are used at each step t to generate the lower-bound KF (LOW-KF), upper-bound KF (HIGH-KF), and DRKF posterior covariance trajectories. To visualize the uncertainty, we use the 95% confidence ellipse $\mathcal{E}(\Sigma) := \{x \in \mathbb{R}^2 : x^\top \Sigma^{-1} x \leq \chi^2_{2,0.95}\}$ with $\chi^2_{2,0.95} = 5.991$. This region contains 95% of a zero-mean Gaussian with covariance Σ . By Theorem 2, $\mathcal{E}(\underline{\Sigma}_{x,t}) \subseteq \mathcal{E}(\Sigma_{x,t}) \subseteq \mathcal{E}(\bar{\Sigma}_{x,t})$.

As shown in Fig. 7, the ellipses at representative time steps confirm the predicted nesting, providing a clear and interpretable robustness envelope.

5.2.2 Convergence Property

Finally, we examine convergence of the time-varying DRKF to its steady-state counterpart using the example from [31]: $A = \begin{bmatrix} 0.1 & 1 \\ 1 & -1 \end{bmatrix}$, $C = [1 \ -1]$,¹⁵ and the ambiguity set radii $\theta_{x_0} = \theta_w = \theta_v = 0.1$. Fig. 9 shows that the relative error between $\text{Tr}[\Sigma_{x,t}]$ and $\text{Tr}[\Sigma_{x,\infty}^*]$ decays approximately linearly on a logarithmic scale, confirming exponential convergence, consistent with the theoretical analysis.

6 Conclusions

We developed a DRKF based on a noise-centric Wasserstein ambiguity model. The proposed formulation preserves the structure of the classical KF, admits explicit spectral bounds, and ensures

¹⁵We set the nominal covariances to $\hat{\Sigma}_w = I_2$ and $\hat{\Sigma}_v = 1$.

dynamic consistency under distributional uncertainty. We established existence, uniqueness, and convergence of the steady-state solution, proved asymptotic minimax optimality, and showed that the steady-state filter is obtained from a single stationary SDP with Kalman-level online complexity. Future directions include extending the framework to nonlinear systems, developing adaptive mechanisms for online calibration of the ambiguity set radius, incorporating model uncertainty in the system matrices, and exploring temporally coupled ambiguity sets.

A Eigenvalue Lower Bounds for DRSE Maximizers

Lemma 5. *Consider the problems (4) and (5) with the explicit eigenvalue lower-bound constraints removed. Then:*

For $t = 0$, (4) admits a maximizer $(\Sigma_{x,0}^{-,}, \Sigma_{v,0}^*)$ such that*

$$\Sigma_{x,0}^{-,*} \succeq \lambda_{\min}(\hat{\Sigma}_{x,0}^-)I_{n_x}, \quad \Sigma_{v,0}^* \succeq \lambda_{\min}(\hat{\Sigma}_{v,0})I_{n_y}. \quad (31)$$

For $t > 0$, (5) admits a maximizer $(\Sigma_{w,t-1}^, \Sigma_{v,t}^*)$ such that*

$$\Sigma_{w,t-1}^* \succeq \lambda_{\min}(\hat{\Sigma}_{w,t-1})I_{n_x}, \quad \Sigma_{v,t}^* \succeq \lambda_{\min}(\hat{\Sigma}_{v,t})I_{n_y}. \quad (32)$$

Proof. For $t = 0$, (31) is shown in [18, Thm. 3.1]. We prove (32) for $t > 0$. Fix $\Sigma_{x,t-1}$, so that $\Sigma_{x,t}^- = A_{t-1}\Sigma_{x,t-1}A_{t-1}^\top + \Sigma_{w,t-1}$. Using the standard identity $\text{Tr}[\Sigma_{x,t}] = \inf_{K_t} \text{Tr}[(I - K_t C_t) \Sigma_{x,t}^- (I - K_t C_t)^\top + K_t \Sigma_{v,t} K_t^\top]$, the objective can be written as

$$\text{Tr}[\Sigma_{x,t}] = \inf_{K_t} \left(\langle (I - K_t C_t)^\top (I - K_t C_t), \Sigma_{w,t-1} \rangle + f_t(K_t, \Sigma_{v,t}) \right),$$

where $\langle A, B \rangle := \text{Tr}[A^\top B]$ and f_t collects the remaining terms (independent of $\Sigma_{w,t-1}$) and is convex and continuous in K_t .

Let $(\bar{\Sigma}_{w,t-1}, \bar{\Sigma}_{v,t})$ be a maximizer of (5) with the explicit eigenvalue bounds removed, which exists since the feasible set (Bures–Wasserstein balls intersected with \mathbb{S}_+) is compact and the objective is continuous. Fixing $\Sigma_{v,t} = \bar{\Sigma}_{v,t}$, the maximization over $\Sigma_{w,t-1}$ matches the setting of [18, Lemma A.3], hence it admits a maximizer $\Sigma_{w,t-1}^* \succeq \lambda_{\min}(\hat{\Sigma}_{w,t-1})I_{n_x}$. Moreover, because $(\bar{\Sigma}_{w,t-1}, \bar{\Sigma}_{v,t})$ is globally optimal, the fixed- $\Sigma_{v,t}$ subproblem achieves the same optimal value, so $(\Sigma_{w,t-1}^*, \bar{\Sigma}_{v,t})$ is also a global maximizer.

Now fix $\Sigma_{w,t-1} = \Sigma_{w,t-1}^*$, which in turn fixes $\Sigma_{x,t}^- = A_{t-1}\Sigma_{x,t-1}A_{t-1}^\top + \Sigma_{w,t-1}^*$. Then, the dependence on $\Sigma_{v,t}$ is of the form $\inf_{K_t} (\langle K_t^\top K_t, \Sigma_{v,t} \rangle + \tilde{f}_t(K_t))$, so applying [18, Lemma A.3] again yields a maximizer $\Sigma_{v,t}^* \succeq \lambda_{\min}(\hat{\Sigma}_{v,t})I_{n_y}$, and $(\Sigma_{w,t-1}^*, \Sigma_{v,t}^*)$ remains globally optimal. This proves (32). \square

B Proofs for Spectral Boundedness

B.1 Proof of Proposition 1

By Lemma 2, there exists $U \in O(n)$ such that $\|X^{1/2} - \hat{X}^{1/2}U\|_F \leq \theta$. Since $\|\cdot\|_2 \leq \|\cdot\|_F$, we also have

$$\|X^{1/2} - \hat{X}^{1/2}U\|_2 \leq \theta. \quad (33)$$

For any matrices $A, B \in \mathbb{R}^{n \times n}$, the singular-value perturbation bounds [36, Cor. 7.3.5] state that

$$\begin{aligned} |\sigma_{\max}(A) - \sigma_{\max}(B)| &\leq \|A - B\|_2 \\ |\sigma_{\min}(A) - \sigma_{\min}(B)| &\leq \|A - B\|_2. \end{aligned} \tag{34}$$

Apply (34) with $A = X^{1/2}$ and $B = \hat{X}^{1/2}U$, and combine with (33) to obtain $|\sigma_{\max}(X^{1/2}) - \sigma_{\max}(\hat{X}^{1/2}U)| \leq \theta$ and $|\sigma_{\min}(\hat{X}^{1/2}U) - \sigma_{\min}(X^{1/2})| \leq \theta$. Because U is orthogonal, $X \succeq 0$ and $\hat{X} \succeq 0$, we have $\sigma_{\max}(\hat{X}^{1/2}U) = \sigma_{\max}(\hat{X}^{1/2}) = \sqrt{\lambda_{\max}(\hat{X})}$ and $\sigma_{\min}(\hat{X}^{1/2}U) = \sigma_{\min}(\hat{X}^{1/2}) = \sqrt{\lambda_{\min}(\hat{X})}$. Substituting these into the inequalities above yields

$$\begin{aligned} \sqrt{\lambda_{\max}(X)} &= \sigma_{\max}(X^{1/2}) \leq \sqrt{\lambda_{\max}(\hat{X})} + \theta, \\ \sqrt{\lambda_{\min}(X)} &= \sigma_{\min}(X^{1/2}) \geq \sqrt{\lambda_{\min}(\hat{X})} - \theta. \end{aligned}$$

Squaring both sides and clipping the lower bound at zero yields the claim.

B.2 Proof of Corollary 2

By Lemma 1, the matrices $\Sigma_{v,t}^*$, $\Sigma_{w,t}^*$ and $\Sigma_{x,0}^{-,*}$ belong to the Bures–Wasserstein balls centered at $\hat{\Sigma}_{v,t}$, $\hat{\Sigma}_{w,t}$ and $\hat{\Sigma}_{x,0}^-$ with radii θ_v , θ_w and θ_{x_0} , respectively. Hence, Proposition 1 gives the corresponding upper bounds.

The lower bounds follow directly from the constraints $\Sigma_{v,t} \succeq \lambda_{\min}(\hat{\Sigma}_{v,t})I_{n_y}$, $\Sigma_{w,t-1} \succeq \lambda_{\min}(\hat{\Sigma}_{w,t-1})I_{n_x}$, and $\Sigma_{x,0}^- \succeq \lambda_{\min}(\hat{\Sigma}_{x,0}^-)I_{n_x}$, which are imposed in (4) and (5). Thus, any maximizers $\Sigma_{v,t}^*$, $\Sigma_{w,t-1}^*$, and $\Sigma_{x,0}^{-,*}$ necessarily satisfy these inequalities, giving the claimed lower bounds.

B.3 Proof of Theorem 2

Define the posterior and prediction maps as

$$\begin{aligned} \Psi(\Sigma_{x,t}^-, \Sigma_{v,t}) &:= \Sigma_{x,t}^- - \Sigma_{x,t}^- C_t^\top (C_t \Sigma_{x,t}^- C_t^\top + \Sigma_{v,t})^{-1} C_t \Sigma_{x,t}^- \\ \Phi(\Sigma_{x,t}, \Sigma_{w,t}) &:= A_t \Sigma_{x,t} A_t^\top + \Sigma_{w,t}. \end{aligned}$$

The DRKF recursion is obtained by evaluating these maps at the least-favorable noise covariances: $\Sigma_{x,t} = \Psi(\Sigma_{x,t}^-, \Sigma_{v,t}^*)$ and $\Sigma_{x,t+1}^- = \Phi(\Sigma_{x,t}, \Sigma_{w,t}^*)$. For $\Sigma_{v,t} \succ 0$, the posterior covariance admits the variational representation

$$\Psi(\Sigma_{x,t}^-, \Sigma_{v,t}) = \inf_{K_t} \left[(I - K_t C_t) \Sigma_{x,t}^- (I - K_t C_t)^\top + K_t \Sigma_{v,t} K_t^\top \right].$$

Hence, Ψ is monotone increasing in each argument: if $\Sigma_{x,t}^{-,(1)} \succeq \Sigma_{x,t}^{-,(2)}$ and $\Sigma_{v,t}^{(1)} \succeq \Sigma_{v,t}^{(2)}$, then for any K_t the corresponding quadratic form is larger, and taking the infimum preserves the Loewner order. The map Φ is also monotone since congruence with A_t and addition of a PSD matrix preserve the Loewner order.

Corollary 2, together with the monotonicity of the posterior and prediction maps Ψ and Φ , implies by induction that, for all $t \geq 0$, the KF driven by $(\underline{\lambda}_{w,t} I_{n_x}, \underline{\lambda}_{v,t} I_{n_y})$ produces covariances no larger than those of the DRKF, and the KF driven by $(\bar{\lambda}_{w,t} I_{n_x}, \bar{\lambda}_{v,t} I_{n_y})$ produces covariances no smaller.

C Proofs for Convergence

C.1 Proof of Lemma 3

By Corollary 2 and Assumption 2, there exist constants $\underline{\lambda}_w, \underline{\lambda}_v > 0$ such that $\Sigma_{w,t}^* \succeq \underline{\lambda}_w I_{n_x} \succ 0$ and $\Sigma_{v,t}^* \succeq \underline{\lambda}_v I_{n_y} \succ 0$. This implies $\Sigma_{w,t}^{N,*} \succ 0$ and $\Sigma_{v,t}^{N,*} \succ 0$, and consequently,

$$\Sigma_{u,t}^N = \mathcal{H}_N \Sigma_{w,t}^{N,*} \mathcal{H}_N^\top + \Sigma_{v,t}^{N,*} \succ 0.$$

Using the matrix inversion lemma, the conditional covariance $\mathcal{Q}_{N,t}$ admits the equivalent representation

$$\mathcal{Q}_{N,t} = ((\Sigma_{w,t}^{N,*})^{-1} + \mathcal{H}_N^\top (\Sigma_{v,t}^{N,*})^{-1} \mathcal{H}_N)^{-1}.$$

Since $(\Sigma_{w,t}^{N,*})^{-1} \succ 0$ and $\mathcal{H}_N^\top (\Sigma_{v,t}^{N,*})^{-1} \mathcal{H}_N \succeq 0$, it follows that $\mathcal{Q}_{N,t} \succ 0$. Moreover, \mathcal{R}_N has full row rank for all $N \geq 1$. Hence, for any nonzero $x \in \mathbb{R}^{n_x}$,

$$x^\top W_{N,t} x = (\mathcal{R}_N^\top x)^\top \mathcal{Q}_{N,t} (\mathcal{R}_N^\top x) > 0,$$

which proves that $W_{N,t} \succ 0$.

Finally, since $\Sigma_{u,t}^N \succ 0$, we have $(\Sigma_{u,t}^N)^{-1} \succ 0$. By Assumption 3, the observability of (A, C) implies that \mathcal{O}_N has full column rank for any $N \geq n_x$. Therefore, for any nonzero $x \in \mathbb{R}^{n_x}$,

$$x^\top \Omega_{N,t} x = (\mathcal{O}_N x)^\top (\Sigma_{u,t}^N)^{-1} (\mathcal{O}_N x) > 0,$$

which establishes $\Omega_{N,t} \succ 0$ for all $N \geq n_x$.

C.2 Proof of Proposition 2

Fix θ_w and θ_v and let $\underline{\lambda}_w := \lambda_{\min}(\hat{\Sigma}_w)$, $\underline{\lambda}_v := \lambda_{\min}(\hat{\Sigma}_v)$, $\bar{\lambda}_w := \bar{\lambda}(\hat{\Sigma}_w, \theta_w)$, and $\bar{\lambda}_v := \bar{\lambda}(\hat{\Sigma}_v, \theta_v)$ as in Corollary 2. Then, the least-favorable covariances satisfy $\underline{\lambda}_w I \preceq \Sigma_{w,t}^{N,*} \preceq \bar{\lambda}_w I$ and $\underline{\lambda}_v I \preceq \Sigma_{v,t}^{N,*} \preceq \bar{\lambda}_v I$. Hence,

$$\Sigma_{u,t}^N = \mathcal{H}_N \Sigma_{w,t}^{N,*} \mathcal{H}_N^\top + \Sigma_{v,t}^{N,*} \preceq (\bar{\lambda}_w \|\mathcal{H}_N\|_2^2 + \bar{\lambda}_v) I,$$

and $\Sigma_{u,t}^N \succeq \underline{\lambda}_v I$. Therefore,

$$\lambda_{\min}(\Omega_{N,t}) \geq \frac{\sigma_{\min}(\mathcal{O}_N)^2}{\lambda_{\max}(\Sigma_{u,t}^N)} \geq \frac{\sigma_{\min}(\mathcal{O}_N)^2}{\bar{\lambda}_v + \bar{\lambda}_w \|\mathcal{H}_N\|_2^2},$$

which implies

$$\|\Omega_{N,t}^{-1}\|_2 \leq \frac{\bar{\lambda}_v + \bar{\lambda}_w \|\mathcal{H}_N\|_2^2}{\sigma_{\min}(\mathcal{O}_N)^2}.$$

Next, using the definition of $\mathcal{G}_{N,t}$, we obtain

$$\|\mathcal{G}_{N,t}\|_2 \leq \|\Sigma_{w,t}^{N,*}\|_2 \|\mathcal{H}_N\|_2 \|(\Sigma_{u,t}^N)^{-1}\|_2 \leq \frac{\bar{\lambda}_w}{\underline{\lambda}_v} \|\mathcal{H}_N\|_2.$$

Consequently,

$$\begin{aligned} \|\alpha_{N,t}\|_2 &\leq \|A^N\|_2 + \|\mathcal{R}_N\|_2 \|\mathcal{G}_{N,t}\|_2 \|\mathcal{O}_N\|_2 \\ &\leq \|A^N\|_2 + \frac{\bar{\lambda}_w}{\underline{\lambda}_v} \|\mathcal{R}_N\|_2 \|\mathcal{H}_N\|_2 \|\mathcal{O}_N\|_2. \end{aligned}$$

Finally, we have that

$$\begin{aligned}\lambda_{\min}(\mathcal{Q}_{N,t}) &\geq \frac{1}{\lambda_{\max}((\Sigma_{w,t}^{N,*})^{-1}) + \lambda_{\max}(\mathcal{H}_N^\top(\Sigma_{v,t}^{N,*})^{-1}\mathcal{H}_N)} \\ &\geq \frac{1}{1/\underline{\lambda}_w + \|\mathcal{H}_N\|_2^2/\underline{\lambda}_v}.\end{aligned}$$

Since $\mathcal{R}_N\mathcal{R}_N^\top \succeq I$, we have $\lambda_{\min}(W_{N,t}) \geq \lambda_{\min}(\mathcal{Q}_{N,t})$, and therefore

$$\|W_{N,t}^{-1}\|_2 \leq 1/\underline{\lambda}_w + \|\mathcal{H}_N\|_2^2/\underline{\lambda}_v.$$

Combining the above bounds yields

$$\|M_{N,t}\|_2 \leq \|\Omega_{N,t}^{-1}\|_2 \|\alpha_{N,t}\|_2^2 \|W_{N,t}^{-1}\|_2 \leq \kappa_N(\theta_v, \theta_w).$$

Substituting into (24) and using the monotonicity of $s \mapsto (\frac{\sqrt{s}}{1+\sqrt{1+s}})^2$ on $s \geq 0$ gives $\xi_{N,t} \leq \bar{\xi}_N(\theta_v, \theta_w)$; inequality (26) then ensures $\xi_{N,t} \leq \rho$ for all $t \geq 0$.

C.3 Proof of Theorem 3

Fix $t \geq 0$ and $N \geq n_x$. By Lemma 3, we have $W_{N,t} \succ 0$ and $\Omega_{N,t} \succ 0$. Hence, the downsampled DR Riccati mapping $r_{\mathbb{D},t}^d$ in (22) is well-defined on $\mathbb{S}_{++}^{n_x}$ and has the robust Riccati form considered in [34, Thm. 5.3]. Therefore, $r_{\mathbb{D},t}^d$ is a strict contraction with respect to Thompson's part metric on $\mathbb{S}_{++}^{n_x}$, with contraction factor $\xi_{N,t} \in (0, 1)$ satisfying the bound (24).

By Proposition 2, we have $\xi_{N,t} \leq \bar{\xi}_N(\theta_v, \theta_w) < 1$ for all $t \geq 0$, and thus $r_{\mathbb{D},t}^d$ is uniformly contractive. Under Assumption 2, the one-step DR Riccati update is stationary, so the downsampled map coincides with the N -fold iterate of a single time-invariant map. The contraction argument for downsampled iterations in [32] then implies that the one-step DR Riccati recursion (19) converges to a unique fixed point $\Sigma_{x,\infty}^- \succ 0$.

Finally, although the stage-wise SDP may admit multiple optimizers in $\Sigma_{v,t}^*$, the corresponding DR Kalman gain is unique. By Lemma 1, for a fixed $\Sigma_{x,t}^-$ the stage-wise DRSE problem amounts to minimizing over K the worst-case posterior MSE, with the adversary maximizing over $\Sigma_{v,t}$ in the SDP's feasible set, denoted by $\mathcal{A}_{v,t}$. Using the standard KF covariance identity, the resulting worst-case one-step MSE is

$$\sup_{\Sigma_{v,t} \in \mathcal{A}_{v,t}} \text{Tr} [(I - KC)\Sigma_{x,t}^-(I - KC)^\top + K\Sigma_{v,t}K^\top].$$

For each feasible $\Sigma_{v,t}$, the associated quadratic map

$$K \mapsto \text{Tr} [(I - KC)\Sigma_{x,t}^-(I - KC)^\top + K\Sigma_{v,t}K^\top]$$

is $\underline{\lambda}_v$ -strongly convex in K (with respect to $\|\cdot\|_F$). Taking the supremum over the compact feasible set $\mathcal{A}_{v,t}$ preserves strong convexity, and hence the minimizer K_t is unique. Moreover, this worst-case objective is continuous in $(\Sigma_{x,t}^-, K)$, so the unique minimizer K_t depends continuously on $\Sigma_{x,t}^-$. Therefore, $\Sigma_{x,t}^- \rightarrow \Sigma_{x,\infty}^-$ implies that the sequence $\{K_t\}$ converges.

C.4 Proof of Corollary 3

For each $t \geq 1$, let $z_t := (\Sigma_{x,t}^-, \Sigma_{x,t}, \Sigma_{w,t-1}^*, \Sigma_{v,t}^*, Y_t, Z_t)$ denote a primal optimal solution of the stage-wise SDP (7). By Theorem 3, $(\Sigma_{x,t}^-, \Sigma_{x,t}) \rightarrow (\Sigma_{x,\infty}^-, \Sigma_{x,\infty})$.

Using the LMIs $\begin{bmatrix} \hat{\Sigma}_w & Y_t \\ Y_t^\top & \Sigma_{w,t-1}^* \end{bmatrix} \succeq 0$ and $\begin{bmatrix} \hat{\Sigma}_v & Z_t \\ Z_t^\top & \Sigma_{v,t}^* \end{bmatrix} \succeq 0$, together with $\hat{\Sigma}_w \succ 0$, $\hat{\Sigma}_v \succ 0$, Schur complements yield $\Sigma_{w,t-1}^* \succeq Y_t^\top \hat{\Sigma}_w^{-1} Y_t$ and $\Sigma_{v,t}^* \succeq Z_t^\top \hat{\Sigma}_v^{-1} Z_t$. Hence, it follows from Corollary 2 that

$$\|Y_t\|_2^2 \leq \|\hat{\Sigma}_w\|_2 \|\Sigma_{w,t-1}^*\|_2 \leq \|\hat{\Sigma}_w\|_2 \bar{\lambda}_w$$

and

$$\|Z_t\|_2^2 \leq \|\hat{\Sigma}_v\|_2 \|\Sigma_{v,t}^*\|_2 \leq \|\hat{\Sigma}_v\|_2 \bar{\lambda}_v,$$

so $\{Y_t\}$ and $\{Z_t\}$ are uniformly bounded. Therefore, $\{z_t\}$ is bounded, and by the Bolzano–Weierstrass theorem, there exists a subsequence t_k such that $z_{t_k} \rightarrow z_\infty$. Writing

$$z_\infty := (\Sigma_{x,\infty}^-, \Sigma_{x,\infty}, \Sigma_{w,\infty}^*, \Sigma_{v,\infty}^*, Y_\infty, Z_\infty),$$

we have $(\Sigma_{w,t_k-1}^*, \Sigma_{v,t_k}^*) \rightarrow (\Sigma_{w,\infty}^*, \Sigma_{v,\infty}^*)$ along this subsequence.

Passing to the limit along this subsequence in the constraints of (7), and using $\Sigma_{x,t_k-1} \rightarrow \Sigma_{x,\infty}$ and the closedness of the PSD cone, shows that z_∞ is feasible for the stationary SDP (13).

We now show that z_∞ is in fact *optimal* for (13). Assume $\theta_w > 0$ and $\theta_v > 0$.¹⁶ Then (13) satisfies Slater’s condition. For instance, choose $\Sigma_{w,\infty} = \hat{\Sigma}_w + \varepsilon I$, $\Sigma_{v,\infty} = \hat{\Sigma}_v + \varepsilon I$, $Y = \hat{\Sigma}_w$, $Z = \hat{\Sigma}_v$, $\Sigma_{x,\infty} = 0$, and $\Sigma_{x,\infty}^- = \Sigma_{w,\infty}$ for sufficiently small $\varepsilon > 0$; this makes all LMIs $\succ 0$ and the trace inequalities strict. Therefore, strong duality holds and the KKT conditions are necessary and sufficient for optimality.

For each $t \geq 1$, let λ_t be a dual optimal solution associated with the primal optimizer z_t of (7) (existence follows from Slater’s theorem). Moreover, since the primal feasible sets are uniformly bounded and Slater’s condition holds, the set of primal–dual optimal pairs is bounded. Thus, after passing to a further subsequence if necessary, we have $\lambda_{t_k} \rightarrow \lambda_\infty$. Taking limits in the KKT conditions of (7) along t_k (all primal/dual feasibility constraints are closed, and complementarity is preserved under limits) yields that $(z_\infty, \lambda_\infty)$ satisfies the KKT conditions of the stationary SDP (13). Consequently, z_∞ is optimal for (13), and $(\Sigma_{x,\infty}^-, \Sigma_{x,\infty}) = (\Sigma_{x,\infty}^{-*}, \Sigma_{x,\infty}^*)$.

Finally, by Theorem 3, the gain sequence $\{K_t\}$ converges. Along the subsequence t_k , $(\Sigma_{x,t_k}^-, \Sigma_{v,t_k}^*) \rightarrow (\Sigma_{x,\infty}^{-*}, \Sigma_{v,\infty}^*)$, and continuity of $K(\Sigma_{x,t}^-, \Sigma_v) = \Sigma_{x,t}^- C^\top (C \Sigma_{x,t}^- C^\top + \Sigma_v)^{-1}$ on $\mathbb{S}_{++}^{n_x} \times \mathbb{S}_{++}^{n_y}$ yields $\lim_{k \rightarrow \infty} K_{t_k} = K_\infty^*$. Since $\{K_t\}$ has a unique limit, we conclude that $K_\infty^* = \lim_{t \rightarrow \infty} K_t$.

D Proofs for Stability and Optimality

D.1 Proof of Theorem 4

Let $\tilde{e}_t := x_t - \bar{x}_t^-$ denote the *prediction* error. From the DRKF update,

$$e_t = x_t - \bar{x}_t = (I - K_\infty^* C) \tilde{e}_t - K_\infty^* (v_t - \hat{v}).$$

The prediction error evolves as $\tilde{e}_t = A e_{t-1} + w_{t-1} - \hat{w}$. Eliminating \tilde{e}_t yields the posterior error recursion

$$\begin{aligned} e_t &= (I - K_\infty^* C) A e_{t-1} + (I - K_\infty^* C) (w_{t-1} - \hat{w}) - K_\infty^* (v_t - \hat{v}) \\ &= F_\infty e_{t-1} + (I - K_\infty^* C) (w_{t-1} - \hat{w}) - K_\infty^* (v_t - \hat{v}). \end{aligned} \tag{35}$$

¹⁶The degenerate case $\theta_w = \theta_v = 0$ reduces to the nominal KF, for which the statement is immediate.

At steady-state, the DRKF covariances satisfy

$$\Sigma_{x,\infty}^{-,*} = A \Sigma_{x,\infty}^* A^\top + \Sigma_{w,\infty}^*$$

with $K_\infty^* = \Sigma_{x,\infty}^{-,*} C^\top (C \Sigma_{x,\infty}^{-,*} C^\top + \Sigma_{v,\infty}^*)^{-1}$. Using the Joseph form,

$$\Sigma_{x,\infty}^* = (I - K_\infty^* C) \Sigma_{x,\infty}^{-,*} (I - K_\infty^* C)^\top + K_\infty^* \Sigma_{v,\infty}^* (K_\infty^*)^\top.$$

Substituting $\Sigma_{x,\infty}^{-,*} = A \Sigma_{x,\infty}^* A^\top + \Sigma_{w,\infty}^*$ gives

$$\Sigma_{x,\infty}^* = F_\infty \Sigma_{x,\infty}^* F_\infty^\top + (I - K_\infty^* C) \Sigma_{w,\infty}^* (I - K_\infty^* C)^\top + K_\infty^* \Sigma_{v,\infty}^* (K_\infty^*)^\top.$$

Hence,

$$\Sigma_{x,\infty}^* - F_\infty \Sigma_{x,\infty}^* F_\infty^\top = Q_\infty,$$

where $Q_\infty := (I - K_\infty^* C) \Sigma_{w,\infty}^* (I - K_\infty^* C)^\top + K_\infty^* \Sigma_{v,\infty}^* (K_\infty^*)^\top$. Since $\Sigma_{w,\infty}^*, \Sigma_{v,\infty}^* \succ 0$, for any $x \neq 0$,

$$x^\top Q_\infty x = \|\Sigma_{w,\infty}^{*,1/2} (I - K_\infty^* C)^\top x\|^2 + \|\Sigma_{v,\infty}^{*,1/2} (K_\infty^*)^\top x\|^2 > 0,$$

which implies $Q_\infty \succ 0$. Thus, $\Sigma_{x,\infty}^* \succ F_\infty \Sigma_{x,\infty}^* F_\infty^\top$. By the standard discrete-time Lyapunov characterization, this strict inequality implies that F_∞ is Schur stable.

Using the temporal independence of $\{w_t\}$ and $\{v_t\}$ and their independence from e_{t-1} , the error covariance $P_t := \text{cov}(e_t)$ satisfies

$$P_t = F_\infty P_{t-1} F_\infty^\top + Q_\infty,$$

whose unique fixed point is $\Sigma_{x,\infty}^*$. Since F_∞ is Schur, $P_t \rightarrow \Sigma_{x,\infty}^*$ and $\sup_{t \geq 0} \mathbb{E}[\|e_t\|^2] < \infty$, completing the proof.

D.2 Proof of Corollary 5

Taking expectations in (35) yields $m_t = F_\infty m_{t-1} + (I - K_\infty^* C)(\mu_w - \hat{w}) - K_\infty^*(\mu_v - \hat{v})$. Since F_∞ is Schur by Theorem 4, we have $\rho(F_\infty) < 1$, and hence $I - F_\infty$ is invertible with $(I - F_\infty)^{-1} = \sum_{k=0}^\infty F_\infty^k$. Therefore, the affine recursion converges, yielding

$$\lim_{t \rightarrow \infty} m_t = (I - F_\infty)^{-1} ((I - K_\infty^* C)(\mu_w - \hat{w}) - K_\infty^*(\mu_v - \hat{v})).$$

If $\hat{w} = \mu_w$ and $\hat{v} = \mu_v$, the constant input term vanishes, and thus $m_t \rightarrow 0$.

D.3 Proof of Theorem 5

For each $t \geq 0$, define the stage-wise minimax value

$$V_t := \inf_{\psi_t \in \mathcal{F}_t} \sup_{\mathbb{P}_{e,t} \in \mathbb{D}_{e,t}} J_t(\psi_t, \mathbb{P}_{e,t}),$$

where $J_t(\psi_t, \mathbb{P}_{e,t})$ is understood almost surely with respect to $\sigma(\mathcal{Y}_{t-1})$. Under Assumption 1, Lemma 1 and Theorem 1 imply that the minimax problem admits a Gaussian least-favorable distribution and that the corresponding optimal estimator is the DRKF ψ_t^* . Moreover, the minimax value is given by $V_t = \text{Tr}[\Sigma_{x,t}]$, where $\Sigma_{x,t} = \Psi(\Sigma_{x,t}^-, \Sigma_{v,t}^*)$ is the DRKF posterior covariance at time t . Consequently, for any admissible estimator $\psi_t \in \mathcal{F}_t$,

$$\sup_{\mathbb{P}_{e,t} \in \mathbb{D}_{e,t}} J_t(\psi_t, \mathbb{P}_{e,t}) \geq V_t = \text{Tr}[\Sigma_{x,t}].$$

Taking $\liminf_{t \rightarrow \infty}$ and using Theorem 3, which guarantees $\Sigma_{x,t} \rightarrow \Sigma_{x,\infty}^*$, yields (27). The corresponding long-run average lower bound (28) follows by Cesàro summability.

We now prove the asymptotic optimality of the steady-state DRKF ψ_∞ with gain K_∞^* . Let $\bar{x}_t^\infty := \psi_\infty(\mathcal{Y}_t)$ and $\bar{x}_t^* := \psi_t^*(\mathcal{Y}_t)$ denote the posterior estimates produced by the steady-state and time-varying DRKFs, respectively. Define the difference $d_t := \bar{x}_t^\infty - \bar{x}_t^*$.

A direct comparison of the measurement updates yields

$$d_t = F_\infty d_{t-1} + \Delta_t \eta_t^*, \quad t \geq 1, \quad (36)$$

where $F_\infty := (I - K_\infty^* C)A$, $\Delta_t := K_\infty^* - K_t$, and $\eta_t^* := y_t - C\bar{x}_t^{-*} - \hat{v}$ is the innovation of the time-varying DRKF. By Theorem 4, F_∞ is Schur, and by Theorem 3 we have $\|\Delta_t\|_2 \rightarrow 0$.

Next, we bound the innovation second moment uniformly. Since $\eta_t^* = C(x_t - \bar{x}_t^{-*}) + (v_t - \hat{v})$,

$$\mathbb{E} [\|\eta_t^*\|^2 | \mathcal{Y}_{t-1}] \leq 2\|C\|_2^2 \mathbb{E} [\|x_t - \bar{x}_t^{-*}\|^2 | \mathcal{Y}_{t-1}] + 2\mathbb{E} [\|v_t - \hat{v}\|^2 | \mathcal{Y}_{t-1}].$$

Under Assumption 2, the ambiguity sets have finite Wasserstein radii, so all $\mathbb{P}_{v,t} \in \mathbb{D}_{v,t}$ have uniformly bounded second moments about \hat{v} . Moreover, Theorem 3 implies $\Sigma_{x,t} \rightarrow \Sigma_{x,\infty}^*$, and hence $\sup_{t \geq 0} \text{Tr}[\Sigma_{x,t}] < \infty$. Since $\Sigma_{x,t}^- = A\Sigma_{t-1}A^\top + \Sigma_{w,t-1}^*$ and $\Sigma_{w,t-1}^* \preceq \bar{\lambda}_w I$ by Corollary 2, it follows that $\sup_{t \geq 0} \text{Tr}[\Sigma_{x,t}^-] < \infty$, and therefore

$$\sup_{t \geq 0} \mathbb{E} [\|x_t - \bar{x}_t^{-*}\|^2 | \mathcal{Y}_{t-1}] < \infty.$$

Consequently, there exists $M_\eta < \infty$ such that

$$\sup_{t \geq 0} \sup_{\mathbb{P}_{e,t} \in \mathbb{D}_{e,t}} \mathbb{E} [\|\eta_t^*\|^2 | \mathcal{Y}_{t-1}] \leq M_\eta.$$

Therefore,

$$\sup_{\mathbb{P}_{e,t} \in \mathbb{D}_{e,t}} \mathbb{E} [\|\Delta_t \eta_t^*\|^2 | \mathcal{Y}_{t-1}] \leq \|\Delta_t\|_2^2 M_\eta \xrightarrow[t \rightarrow \infty]{} 0.$$

Since F_∞ is Schur, iterating (36) and using the above uniform bound yields that $d_t \rightarrow 0$ in mean square; in particular,

$$D_t := \sup_{\mathbb{P}_{e,t} \in \mathbb{D}_{e,t}} \mathbb{E} [\|d_t\|^2 | \mathcal{Y}_{t-1}] \xrightarrow[t \rightarrow \infty]{} 0.$$

Let $e_t^* := x_t - \bar{x}_t^*$ denote the time-varying DRKF posterior error. Since $x_t - \bar{x}_t^\infty = e_t^* - d_t$, we have

$$\|x_t - \bar{x}_t^\infty\|^2 \leq \|e_t^*\|^2 + \|d_t\|^2 + 2\|e_t^*\|\|d_t\|.$$

Taking conditional expectations and then the supremum over $\mathbb{D}_{e,t}$ yields

$$\sup_{\mathbb{P}_{e,t} \in \mathbb{D}_{e,t}} J_t(\psi_\infty, \mathbb{P}_{e,t}) \leq \sup_{\mathbb{P}_{e,t} \in \mathbb{D}_{e,t}} J_t(\psi_t^*, \mathbb{P}_{e,t}) + D_t + 2\sqrt{D_t} \sqrt{\sup_{\mathbb{P}_{e,t} \in \mathbb{D}_{e,t}} J_t(\psi_t^*, \mathbb{P}_{e,t})}.$$

By stage-wise minimax optimality of the time-varying DRKF, $\sup_{\mathbb{P}_{e,t} \in \mathbb{D}_{e,t}} J_t(\psi_t^*, \mathbb{P}_{e,t}) = V_t = \text{Tr}[\Sigma_{x,t}]$. Thus,

$$\sup_{\mathbb{P}_{e,t} \in \mathbb{D}_{e,t}} J_t(\psi_\infty, \mathbb{P}_{e,t}) \leq V_t + D_t + 2\sqrt{V_t} \sqrt{D_t}. \quad (37)$$

Taking $\limsup_{t \rightarrow \infty}$ and using $D_t \rightarrow 0$ and $V_t \rightarrow \text{Tr}[\Sigma_{x,\infty}^*]$ gives

$$\limsup_{t \rightarrow \infty} \sup_{\mathbb{P}_{e,t} \in \mathbb{D}_{e,t}} J_t(\psi_\infty, \mathbb{P}_{e,t}) \leq \text{Tr}[\Sigma_{x,\infty}^*].$$

Combined with the lower bound (27) applied to ψ_∞ , this proves (29). The Cesàro-average optimality statement (30) follows similarly since $\sup_t V_t < \infty$ and $D_t \rightarrow 0$ imply $\frac{1}{T} \sum_{t=0}^{T-1} D_t \rightarrow 0$, and hence all error terms in (37) have vanishing Cesàro mean.

References

- [1] M. Jang, A. Hakobyan, and I. Yang, “On the steady-state distributionally robust Kalman filter,” *arXiv preprint arXiv:2503.23742*, 2025.
- [2] R. E. Kalman, “A new approach to linear filtering and prediction problems,” *J. Basic Eng.*, vol. 82, pp. 35–45, 1960.
- [3] D. Simon, *Optimal State Estimation: Kalman, H_∞ , and Nonlinear Approaches*. John Wiley & Sons, 2006.
- [4] J. L. Speyer, C.-H. Fan, and R. N. Banavar, “Optimal stochastic estimation with exponential cost criteria,” in *Proc. IEEE Conf. Decis. Control*, 1992, pp. 2293–2299.
- [5] P. Whittle, “Risk-sensitive linear/quadratic/Gaussian control,” *Adv. Appl. Probab.*, vol. 13, no. 4, pp. 764–777, 1981.
- [6] B. P. Van Parys, D. Kuhn, P. J. Goulart, and M. Morari, “Distributionally robust control of constrained stochastic systems,” *IEEE Trans. Autom. Control*, vol. 61, no. 2, pp. 430–442, 2015.
- [7] I. Yang, “Wasserstein distributionally robust stochastic control: A data-driven approach,” *IEEE Trans. Autom. Control*, vol. 66, no. 8, pp. 3863–3870, 2021.
- [8] M. Schuurmans and P. Patrinos, “A general framework for learning-based distributionally robust MPC of Markov jump systems,” *IEEE Trans. Autom. Control*, 2023.
- [9] B. Li, T. Guan, L. Dai, and G.-R. Duan, “Distributionally robust model predictive control with output feedback,” *IEEE Trans. Autom. Control*, vol. 69, no. 5, pp. 3270–3277, 2024.
- [10] A. Hakobyan and I. Yang, “Wasserstein distributionally robust control of partially observable linear stochastic systems,” *IEEE Trans. Autom. Control*, vol. 69, no. 9, pp. 6121–6136, 2024.
- [11] R. D. McAllister and P. M. Esfahani, “Distributionally robust model predictive control: Closed-loop guarantees and scalable algorithms,” *IEEE Trans. Autom. Control*, vol. 70, no. 5, pp. 2963–2978, 2025.
- [12] J.-S. Brouillon, A. Martin, J. Lygeros, F. Dörfler, and G. F. Trecate, “Distributionally robust infinite-horizon control: from a pool of samples to the design of dependable controllers,” *IEEE Trans. Autom. Control*, vol. 70, no. 10, pp. 6465–6480, 2025.
- [13] S. Wang, Z. Wu, and A. Lim, “Robust state estimation for linear systems under distributional uncertainty,” *IEEE Trans. Signal Process.*, vol. 69, pp. 5963–5978, 2021.
- [14] S. Wang and Z.-S. Ye, “Distributionally robust state estimation for linear systems subject to uncertainty and outlier,” *IEEE Trans. Signal Process.*, vol. 70, pp. 452–467, 2021.
- [15] M. Zorzi, “Robust Kalman filtering under model perturbations,” *IEEE Trans. Autom. Control*, vol. 62, no. 6, pp. 2902–2907, 2016.
- [16] B. C. Levy and R. Nikoukhah, “Robust state space filtering under incremental model perturbations subject to a relative entropy tolerance,” *IEEE Trans. Autom. Control*, vol. 58, no. 3, pp. 682–695, 2012.

- [17] S. Shafieezadeh Abadeh, V. A. Nguyen, D. Kuhn, and P. M. Mohajerin Esfahani, “Wasserstein distributionally robust Kalman filtering,” *Adv. Neural Inf. Process. Syst.*, vol. 31, 2018.
- [18] V. A. Nguyen, S. Shafieezadeh-Abadeh, D. Kuhn, and P. Mohajerin Esfahani, “Bridging Bayesian and minimax mean square error estimation via Wasserstein distributionally robust optimization,” *Math. Oper. Res.*, vol. 48, no. 1, pp. 1–37, 2023.
- [19] K. Lotidis, N. Bambos, J. Blanchet, and J. Li, “Wasserstein distributionally robust linear-quadratic estimation under martingale constraints,” in *Proc. Int. Conf. Artif. Intell. Stat.* PMLR, 2023, pp. 8629–8644.
- [20] B. Han, “Distributionally robust Kalman filtering with volatility uncertainty,” *IEEE Trans. Autom. Control*, vol. 70, no. 6, pp. 4000–4007, 2025.
- [21] T. Kargin, J. Hajar, V. Malik, and B. Hassibi, “Distributionally robust Kalman filtering over finite and infinite horizon,” *arXiv preprint arXiv:2407.18837*, 2024.
- [22] B. D. Anderson and J. B. Moore, *Optimal Filtering*. Courier Corporation, 2005.
- [23] R. Mehra, “On the identification of variances and adaptive Kalman filtering,” *IEEE Trans. Autom. Control*, vol. 15, no. 2, pp. 175–184, 1970.
- [24] B. J. Odelson, M. R. Rajamani, and J. B. Rawlings, “A new autocovariance least-squares method for estimating noise covariances,” *Automatica*, vol. 42, no. 2, pp. 303–308, 2006.
- [25] P. Mohajerin Esfahani and D. Kuhn, “Data-driven distributionally robust optimization using the Wasserstein metric: Performance guarantees and tractable reformulations,” *Math. Program.*, vol. 171, no. 1–2, pp. 115–166, 2018.
- [26] R. Gao and A. Kleywegt, “Distributionally robust stochastic optimization with Wasserstein distance,” *Math. Oper. Res.*, vol. 48, no. 2, pp. 603–655, 2023.
- [27] M. Gelbrich, “On a formula for the L2 Wasserstein metric between measures on Euclidean and Hilbert spaces,” *Mathematische Nachrichten*, vol. 147, no. 1, pp. 185–203, 1990.
- [28] A. Nemirovski, “Interior point polynomial time methods in convex programming,” *Lecture Notes*, vol. 42, no. 16, pp. 3215–3224, 2004.
- [29] R. Bhatia, T. Jain, and Y. Lim, “On the Bures–Wasserstein distance between positive definite matrices,” *Expositiones Mathematicae*, vol. 37, no. 2, pp. 165–191, 2019.
- [30] D. Jacobson, “Optimal stochastic linear systems with exponential performance criteria and their relation to deterministic differential games,” *IEEE Trans. Autom. Control*, vol. 18, no. 2, pp. 124–131, 1973.
- [31] M. Zorzi and B. C. Levy, “On the convergence of a risk sensitive like filter,” in *Proc. IEEE Conf. Decis. Control*, 2015, pp. 4990–4995.
- [32] M. Zorzi, “Convergence analysis of a family of robust Kalman filters based on the contraction principle,” *SIAM J. Control Optim.*, vol. 55, no. 5, pp. 3116–3131, 2017.
- [33] B. C. Levy and M. Zorzi, “A contraction analysis of the convergence of risk-sensitive filters,” *SIAM J. Control Optim.*, vol. 54, no. 4, pp. 2154–2173, 2016.

- [34] H. Lee and Y. Lim, "Invariant metrics, contractions and nonlinear matrix equations," *Nonlinearity*, vol. 21, no. 4, p. 857, 2008.
- [35] R. Gao, X. Chen, and A. J. Kleywegt, "Wasserstein distributionally robust optimization and variation regularization," *Oper. Res.*, vol. 72, no. 3, pp. 1177–1191, 2024.
- [36] R. A. Horn and C. R. Johnson, *Matrix Analysis*, 2nd ed. Cambridge University Press, 2012.